Properties of constraint-based single-point approximate kinetic energy functionals

V. V. Karasiev,[1,2,*] R. S. Jones,[3] S. B. Trickey,[2,†] and Frank E. Harris[2,4]
[1]*Centro de Química, Instituto Venezolano de Investigaciones Científicas, Apartado 21827, Caracas 1020-A, Venezuela*
[2]*Quantum Theory Project, Departments of Physics and of Chemistry, University of Florida, Gainesville, Florida 32611, USA*
[3]*Department of Physics, Loyola College in Maryland, 4501 N. Charles Street, Baltimore, Maryland 21210, USA*
[4]*Department of Physics, University of Utah, Salt Lake City, Utah, 84112 USA*
(Received 10 September 2008; revised manuscript received 6 November 2009; published 31 December 2009)

We present an analysis and extension of our constraint-based approach to orbital-free (OF) kinetic-energy (KE) density functionals intended for the calculation of quantum-mechanical forces in multiscale molecular-dynamics simulations. Suitability for realistic system simulations requires that the OF-KE functional yield accurate forces on the nuclei yet be computationally simple. We therefore require that the functionals be based on density-functional theory constraints, be local, be dependent at most upon a small number of parameters fitted to a training set of limited size, and be applicable beyond the scope of the training set. Our previous "modified-conjoint" generalized-gradient-type functionals were constrained to producing a positive-definite Pauli potential. Though distinctly better than several published generalized-gradient-approximation-type functionals in that they gave semiquantitative agreement with Born-Oppenheimer forces from full Kohn-Sham results, those modified-conjoint functionals suffer from unphysical singularities at the nuclei. Here we show how to remove such singularities by introducing higher-order density derivatives and analyze the consequences. We give a simple illustration of such a functional and a few tests of it.

DOI: 10.1103/PhysRevB.80.245120 PACS number(s): 71.15.Mb, 31.15.xv

I. INTRODUCTION

Simulation of the structure and properties of complicated materials is a demanding task, particularly away from equilibrium, for example, in the simultaneous presence of solvents and mechanical stress. Though the present results are not limited to it, our motivating problem has been tensile fracture of silica in the presence of water.

For such problems, quantum-mechanical treatment of the reactive zone is essential at least at the level of realistic Born-Oppenheimer (B-O) forces to drive an otherwise classical molecular-dynamics (MD) or molecular mechanics (MM) calculation. Computational cost then leads to a nested-region strategy. Internuclear forces in the reactive zone are obtained from an explicitly quantum-mechanical treatment. Forces between other nuclei are calculated from classical potentials. Such partitioning is called multiscale simulation in the computational materials community and QM/MD (or QM/MM) methodology in computational molecular biology.

The QM calculation is the computationally rate-limiting step. QM approximations good enough yet computationally fast on the scale of the MD algorithms are therefore critical. Both the inherent form and the growing dominance of density-functional theory (DFT) for describing molecular, biomolecular, and materials systems make it a reasonable candidate QM. Despite advances in pseudopotentials and order-N approximations, however, solution of the DFT Kohn-Sham (KS) problem is too slow computationally to be fully satisfactory. An alternative, Car-Parrinello dynamics,[1] does not guarantee that the motion is restricted to the B-O energy surface.

Thus, there is continuing need for methods which yield essentially full DFT accuracy at significantly lower computational cost. In response, we and co-workers proposed and demonstrated a graded sequence of approximations[2] scheme. Its essence is use of a simple classical potential for the majority of MD steps, with periodic correction by calibration to forces obtained from more accurate but slower methods. An example graded sequence of approximations would be as follows: (1) classical potential; (2) simple reactive (charge redistribution) potential;[3–5] (3) orbital-free (OF) DFT, the subject of this paper; (4) quasi-spin-density DFT (Ref. 6) (a way to approximate spin-dependent effects at the cost of non-spin-polarized KS-DFT); (5) full spin-polarized DFT (the level of refinement ultimately required for bond breaking).

In this hierarchy, a large gap in computational cost separates reactive potentials and quasi-spin-density DFT. Since the cost of conventional KS calculations comes from solving for the KS orbitals, an obvious candidate to fill the gap is listed: OF-DFT. The long-standing barrier is a lack of an effective OF approximation to the kinetic energy (KE). Background and a description of our first OF-KE functionals were reported in a paper addressed to the computational materials science community,[7] with a more didactic survey in Ref. 8. The present analysis focuses on identifying the causes of limitations of those functionals and ways to eliminate those limitations.

II. BACKGROUND AND BASICS

Construction of an accurate, explicit, total electronic kinetic energy density functional $T[n]=\langle\Psi|\hat{T}|\Psi\rangle$ for a many-electron system in state $|\Psi\rangle$ with electron number density n is an unresolved task.[9–11] The Coulomb virial theorem suggests that the task is equivalent to seeking the total energy functional itself. The Kohn-Sham KE is thus a more attractive target for multiple reasons. Of course, the appeal of OF-DFT predates modern DFT, as witness the Thomas-Fermi-Dirac[12,13] and von Weizsäcker[14] models.

There has been considerable activity more recently. A review with extensive references is given in Ref. 15. Other relevant work is that of Carter and co-workers; a helpful review with many references is Ref. 16. More recent developments include, for example, Refs. 17–22 as well as our own work already cited.

Distinct from most other recent efforts, our approach is to construct *one-point*, *i.e., local*, approximate KE functionals specifically for MD computations. We insist on constraint-based forms and parameters, that is, satisfaction of known exact results for positivity, scaling, and the like. We are willing, as needed, to simplify the search by requiring only that the functional give adequate interatomic forces, not total energies (and certainly not KS band structures nor general linear response).

To summarize basics and set notation, the Kohn-Sham[23] kinetic energy T_s, the major contribution to T, is defined in terms of the KS orbitals (Hartree atomic units unless otherwise noted):

$$T_s[\{\phi_i\}_{i=1}^N] = \sum_{i=1}^N \int \phi_i^*(\mathbf{r})\left(-\frac{1}{2}\nabla^2\right)\phi_i(\mathbf{r})d^3\mathbf{r} \equiv \int t_{\text{orb}}(\mathbf{r})d^3\mathbf{r}. \tag{1}$$

Although $T_s > 0$, t_{orb} is not necessarily greater than zero. It is preferable, therefore, to use the equivalent form

$$t_s \equiv t_{\text{orb}} + \frac{1}{4}\nabla^2 n, \tag{2}$$

which is positive definite.[24]

The remainder, $T - T_s$, is included in the exchange-correlation (XC) functional $E_{xc}[n]$. Since successful E_{xc} approximations assume this KS KE decomposition, we focus on T_s. This approach also evades the formidable task associated with the full $T[n]$ just mentioned.

For $T_s[n]$ an explicit functional of n, the DFT total energy functional is orbital-free:

$$E^{\text{OF-DFT}}[n] = T_s[n] + E_{\text{Ne}}[n] + E_{\text{H}}[n] + E_{xc}[n] + E_{\text{NN}}. \tag{3}$$

Here $E_{\text{Ne}}[n]$ is the nuclear-electron interaction energy functional, $E_{\text{H}}[n]$ is the Hartree functional (classical electron-electron repulsion), and E_{NN} is the internuclear repulsion. Then the variational principle gives the single Euler equation

$$\frac{\delta T_s[n]}{\delta n(\mathbf{r})} + v_{\text{KS}}([n];\mathbf{r}) = \mu, \tag{4}$$

where μ is the Lagrange multiplier for density normalization $\int n(\mathbf{r})d^3\mathbf{r} = N$ at the nuclear configuration $\mathbf{R}_1, \mathbf{R}_2, \ldots$, and $v_{\text{KS}} = \delta(E_{\text{Ne}} + E_{\text{H}} + E_{xc})/\delta n$. The force on nucleus I at $\mathbf{R}_I$ is simply

$$\mathbf{F}_I = -\nabla_{\mathbf{R}_I} E^{\text{OF-DFT}} = -\nabla_{\mathbf{R}_I} E_{\text{NN}} - \int n(\mathbf{r})\nabla_{\mathbf{R}_I} v_{\text{Ne}} d^3\mathbf{r} - \int \left[\frac{\delta T_s[n]}{\delta n(\mathbf{r})} + v_{\text{KS}}([n];\mathbf{r})\right]\nabla_{\mathbf{R}_I} n(\mathbf{r})d^3\mathbf{r}. \tag{5}$$

The third term in Eq. (5) shows that the biggest error in the calculated force will come from the gradient of the approximate $T_s[n]$ functional, because the kinetic energy is an order of magnitude larger than the magnitude of E_{xc} (which also must be approximated in practice). As will be discussed, when the development of approximate KE functionals focuses on forces, it is convenient to use Eq. (5) with number density $n(\mathbf{r})$ from a conventional KS calculation (with a specific approximate E_{xc}) as input.

In constructing approximate functionals it is quite common to begin with the Thomas-Fermi (TF) functional,[12,13]

$$T_{\text{TF}}[n] = c_0 \int n^{5/3}(\mathbf{r})d^3\mathbf{r} \equiv \int t_0(\mathbf{r})d^3\mathbf{r},$$

$$c_0 = \frac{3}{10}(3\pi^2)^{2/3}. \tag{6}$$

By itself, the TF functional is not an acceptable approximation, because of, for example, the Teller nonbinding theorem.[25] A more productive route for our purposes is to decompose $T_s[n]$ into the von Weizsäcker energy T_{W},[14] plus a *non-negative* remainder, known as the Pauli term T_θ,[26–29]

$$T_s[n] = T_{\text{W}}[n] + T_\theta[n], \quad T_\theta[n] \geq 0, \tag{7}$$

with

$$T_{\text{W}}[n] = \frac{1}{8}\int \frac{|\nabla n(\mathbf{r})|^2}{n(\mathbf{r})}d^3\mathbf{r} \equiv \int t_{\text{W}}[n(\mathbf{r})]d^3\mathbf{r}. \tag{8}$$

As analyzed in detail below, the non-negativity of T_θ and $t_\theta(\mathbf{r})$ defined by

$$T_\theta = \int t_\theta(\mathbf{r})d^3\mathbf{r},$$

$$t_\theta := t_s - \sqrt{n}\frac{1}{2}\nabla^2\sqrt{n} \tag{9}$$

is a crucial but not sufficient condition for determining a realistic OF-KE approximation.[7] Details of the consequences of enforcing that condition are a focus of this paper.

III. GGA-TYPE KE FUNCTIONALS AND THEIR LIMITATIONS

A. Basic structure

Pursuit of single-point approximations for $t_s(\mathbf{r}) = t_{\text{W}}[n(\mathbf{r}), \nabla n(\mathbf{r})] + t_\theta[n(\mathbf{r}), \nabla n(\mathbf{r}), \ldots]$ stimulates consideration of a counterpart to the generalized gradient approximation (GGA) for XC,[30] namely,

$$T_s^{\text{GGA}}[n] = c_0 \int n^{5/3}(\mathbf{r})F_t[s(\mathbf{r})]d^3\mathbf{r}. \tag{10}$$

Here s is a dimensionless reduced density gradient

$$s \equiv \frac{|\nabla n|}{2nk_F}, \quad k_F \equiv (3\pi^2 n)^{1/3}. \tag{11}$$

F_t is a kinetic energy enhancement factor which goes to unity for uniform density. Equation (10) is motivated in part by the

conjointness conjecture,[31] which posits that $F_t(s) \propto F_x(s)$, where F_x is the enhancement factor in GGA exchange. We showed previously that this relationship cannot hold strictly,[7] but the form is suggestive and useful.

For connection with $T_\theta \geq 0$, we re-express T_W in a form parallel with Eq. (10). From Eqs. (7), (8), and (11),

$$T_W[n] = c_0 \int n^{5/3}(\mathbf{r}) \frac{5}{3} s^2(\mathbf{r}) d^3\mathbf{r}, \tag{12}$$

$$T_s^{GGA}[n] = T_W[n] + c_0 \int n^{5/3}(\mathbf{r}) F_\theta[s(\mathbf{r})] d^3\mathbf{r}, \tag{13}$$

where

$$F_\theta(s) = F_t(s) - \frac{5}{3} s^2. \tag{14}$$

The final term of Eq. (13) thus is a formal representation of the GGA Pauli term T_θ^{GGA}. Note that the form of Eq. (13) automatically preserves proper uniform scaling of T_s (see Ref. 32):

$$T_s[n_\gamma] = \gamma^2 T_s[n],$$

$$n_\gamma(\mathbf{r}) := \gamma^3 n(\gamma \mathbf{r}). \tag{15}$$

Constraints that must be satisfied by the enhancement factors associated with any satisfactory GGA KE functional include

$$t_\theta([n];\mathbf{r}) \geq 0, \tag{16}$$

as well as[29,33,34]

$$v_\theta([n];\mathbf{r}) = \delta T_\theta[n]/\delta n(\mathbf{r}) \geq 0, \quad \forall \quad \mathbf{r}. \tag{17}$$

The quantity v_θ is known as the Pauli potential. Constraint Eq. (16) implies the non-negativity of the GGA enhancement factor, $F_\theta[s(\mathbf{r})] \geq 0$.

For a slowly varying density that is not itself small, we have $s \approx 0$, and it is appropriate to write T_s as a gradient expansion:[35]

$$T_s[n] = T_{TF}[n] + \frac{1}{9} T_W[n] + \text{higher-order terms}. \tag{18}$$

Truncation at second order in s gives the second-order gradient approximation (SGA), with the SGA enhancement factor[30]

$$F_t^{SGA}(s) = 1 + \frac{1}{9} \cdot \frac{5}{3} s^2 = 1 + \frac{5}{27} s^2 \tag{19}$$

or

$$F_\theta^{SGA}(s) = 1 - \frac{40}{27} s^2. \tag{20}$$

These forms should be exhibited by the exact functional in the limit of small density variation. (Though there are $s \to \infty$ constraints,[11] we have not used them so far.)

For GGA functionals, v_θ, Eq. (17), can be written[36,37] as

$$\frac{\delta T_\theta^{GGA}}{\delta n(\mathbf{r})} = \frac{\partial t_\theta[n(\mathbf{r}), \nabla n(\mathbf{r})]}{\partial n(\mathbf{r})} - \nabla \cdot \frac{\partial t_\theta[n(\mathbf{r}), \nabla n(\mathbf{r})]}{\partial [\nabla n(\mathbf{r})]}. \tag{21}$$

After some tedium, one finds

$$v_\theta^{GGA} = \frac{5}{3} c_0 n^{2/3} F_\theta + c_0 n^{5/3} \frac{\partial F_\theta}{\partial s} \left[\frac{\partial s}{\partial n} - \frac{5}{3} \frac{\nabla n}{n} \cdot \frac{\partial s}{\partial \nabla n} - \nabla \cdot \frac{\partial s}{\partial \nabla n} \right] - c_0 n^{5/3} \frac{\partial^2 F_\theta}{\partial s^2} \left(\nabla s \cdot \frac{\partial s}{\partial \nabla n} \right). \tag{22}$$

[The last line was omitted in Eq. (34) of Ref. 7 but included in the actual numerical work.] A somewhat cleaner expression that also facilitates understanding the extension presented below comes from shifting to the variable s^2 and defining both the reduced Laplacian density p,

$$p \equiv \frac{\nabla^2 n}{(2k_F)^2 n} = \frac{\nabla^2 n}{4(3\pi^2)^{2/3} n^{5/3}}, \tag{23}$$

and one of the various possible dimensionless fourth-order derivatives q,

$$q \equiv \frac{\nabla n \cdot (\nabla \nabla n) \cdot \nabla n}{(2k_F)^4 n^3} = \frac{\nabla n \cdot (\nabla \nabla n) \cdot \nabla n}{16(3\pi^2)^{4/3} n^{13/3}}. \tag{24}$$

(Note that our s^2, p correspond to p, q, respectively, in Ref. 19.) Then Eq. (22) becomes

$$v_\theta^{GGA}(s^2) = c_0 n^{2/3} \left\{ \frac{5}{3} F_\theta(s^2) - \left(\frac{2}{3} s^2 + 2p \right) \frac{\partial F_\theta}{\partial (s^2)} + \left(\frac{16}{3} s^4 - 4q \right) \frac{\partial^2 F_\theta}{\partial (s^2)^2} \right\}. \tag{25}$$

See Appendix A for details.

B. Singularities

Near a point nucleus of charge Z at the origin, the number density behaves to first order in r as

$$n(\mathbf{r}) \sim (1 - 2Z|\mathbf{r}|) + O(|\mathbf{r}|^2), \tag{26}$$

as required by Kato's cusp condition.[38–42] Sufficiently close to a nucleus, therefore, $n(\mathbf{r})$ behaves as a hydrogenlike $1s$-electron density

$$n_H(\mathbf{r}) \sim \exp(-2Z|\mathbf{r}|). \tag{27}$$

That is, the variation in $n'(r)/n(r)$ is equal for these densities sufficiently close to the nucleus, hence, the form in Eq. (27) is a reasonable near-nucleus approximation.[43] Consequences of differences in the higher-order terms in the respective Taylor expansions of actual and hydrogenic $1s$ densities are discussed in Sec. IV A. See Refs. 29 and 44 for related discussions.

For $n(\mathbf{r})$ of the form of Eq. (27) at $r=0$, s and q remain finite while $p \to -4Z/(2k_F)^2 r$. In this case, Eq. (25) becomes

$$v_\theta^{\mathrm{GGA}}(r\to 0)=\frac{3Z}{5r}\frac{\partial F_\theta^{\mathrm{GGA}}}{\partial(s^2)}+\text{nonsingular terms}. \quad (28)$$

If s^2 is sufficiently small that it is a good approximation to write $F_\theta^{\mathrm{GGA}}\approx 1+as^2$ (note that this is exactly the form of F_θ^{SGA}), Eq. (28) simplifies to

$$v_\theta^{\mathrm{GGA}}(r\to 0)=\frac{3aZ}{5r}+\text{nonsingular terms}, \quad (29)$$

in which case v_θ^{GGA} tends to infinity at the nuclei with the same sign as the GGA parameter a. The small values of s^2 at the nuclei make this a general phenomenon. [Near typical nuclei ($r\to 0$), numerical experience shows that $s^2\approx 0.15$, so that the small-s^2 behavior of any $F_\theta(s^2)$ of GGA form is relevant there.]

Equation (29) shows that purely GGA Pauli potentials have singularities in the vicinity of nuclear sites. In contrast, calculations using KS quantities as inputs show that the exact Pauli potential is finite at the nuclei (see, for example, Ref. 27 as well as Fig. 2). Moreover, the positivity requirement for v_θ will certainly be violated near the nuclei both for F_θ^{SGA} and for any GGA form with $a<0$.

C. Positivity: tests and enforcement

To assess these positivity constraints, we tested six published KE functionals[45–50] that either are strictly conjoint or are based closely on conjointness. The test used the diatomic molecule SiO, an important reference species for us. With local-density approximation (LDA) XC, we did a conventional orbital-dependent KS calculation as a function of bond length (details are in Appendix B). At each bond length, the converged KS density was used as input to the orbital-free $E[n]$ corresponding to one of the six $T_s[n]$ approximations. None of the six gave a stable SiO molecule. All six produced $a\le 0$ in Eq. (29); hence, all six have nontrivial violations of v_θ positivity. In fact, all the effective enhancement factors are very close to that of the SGA, $F_\theta(s)=1-40/27s^2$. Details are in Refs. 7 and 8. Because of the constraint violation, conjointness can at most be a guide.

We enforced positivity of v_θ^{GGA} by particular parametrization of two $F_t(s)$ forms. One is based on the Perdew, Burke, and Ernzerhof (PBE) (Ref. 46) GGA XC form

$$F_t^{\mathrm{PBE}\nu}(s)=1+\sum_{i=1}^{\nu-1}C_i\left[\frac{s^2}{1+a_1s^2}\right]^i,\quad \nu=2,3,4,$$

$$F_t^{\exp 4}(s)=C_1(1-e^{-a_1s^2})+C_2(1-e^{-a_2s^4}). \quad (30)$$

Our PBE2 form is identical (but with different parameters) to the form used by Tran and Wesolowski.[45] Our PBE3 corresponds to the form introduced by Adamo and Barone,[47] but, again, with different parameters. Quite similar forms also were explored by King and Handy[51] in the context of directly fitting a KS kinetic potential $v_s=\delta T_s/\delta n$ to conventional KS eigenvalues and orbitals; see Eq. (34) below.

We fitted the parameters in the enhancement factors, Eq. (30), to match the conventional KS internuclear forces for various nuclear configurations of a three-molecule training set: SiO, H_4SiO_4, and $H_6Si_2O_7$. With conventional KS densities as input, we found semiquantitative agreement with the conventional KS calculations for single bond stretching in H_4SiO_4, $H_6Si_2O_7$, H_2O, CO, and N_2. All had energy minima within 5%–20% of the conventional KS equilibrium bond-length values. The latter two molecules were particularly encouraging, since no data on C or N was included in the parametrization. Details, including parameter values, are in Ref. 7.

D. Analysis of fitted functional behavior

Despite this progress, there is a problem. Although the PBEν and exp4 forms give Pauli potentials that are everywhere positive, yielding $a>0$ in Eq. (29), they are singular at the nuclei, in contrast to the negative singularities of previously published forms. For clarity about the developments which follow, observe that these nuclear-site singularities occur in v_θ, hence, are distinct from the intrinsic nuclear-site singularity of the von Weizsäcker potential, which by operation on Eq. (8) can be shown to be

$$v_{\mathrm{W}}\equiv\frac{\delta T_{\mathrm{W}}[n]}{\delta n(\mathbf{r})}=\frac{1}{8}\left[\frac{|\nabla n|^2}{n^2}-\frac{2\nabla^2 n}{n}\right]. \quad (31)$$

The intrinsic singularity of v_{W} near a nucleus follows from Eq. (26) as

$$v_{\mathrm{W}}=-\frac{2Z}{r}. \quad (32)$$

Insight regarding the behavior of our modified-conjoint functionals can be gained from consideration of the energy density $dT_\theta^{\mathrm{approx}}(s)/ds$ as a function of s for various functionals indicated by the generic superscript "approx." This quantity comes from differentiation of the integrated contribution $T_\theta^{\mathrm{approx}}(s)$ of the region $s(\mathbf{r})\le s$ to the kinetic energy:

$$T_\theta^{\mathrm{approx}}(s)\equiv\int_{s(\mathbf{r})\le s}t_\theta^{\mathrm{approx}}([n];\mathbf{r})d^3\mathbf{r}$$
$$=\int_0^s ds\int t_\theta^{\mathrm{approx}}([n];\mathbf{r})\delta[s-s(\mathbf{r})]d^3\mathbf{r}. \quad (33)$$

Figure 1 shows $dT_\theta^{\mathrm{approx}}(s)/ds$ for the SiO molecule at bond length $R=1.926$ Å (slightly stretched). Values are shown for the PBE2 parametrization (that respects positivity), the Tran-Wesolowski parametrization of the same form (PBE-TW), and for the exact orbital-dependent KS Pauli term calculated from[29]

$$t_\theta^{\mathrm{KS}}=t_s-\left(\frac{1}{8}\frac{|\nabla n|^2}{n}-\frac{1}{4}\nabla^2 n\right), \quad (34)$$

where t_θ and t_s are defined in Eqs. (9) and (2), respectively.

Figure 1 also shows that both approximate functionals closely resemble the exact KS kernel for $0.24<s<0.38$. But both of them have a much larger second peak around $s\approx 0.5$. In contrast, the exact functional actually has a long low region before a second peak at $s\approx 0.9$. PBE2 mimics the true second peak via a too-strong third peak while the con-

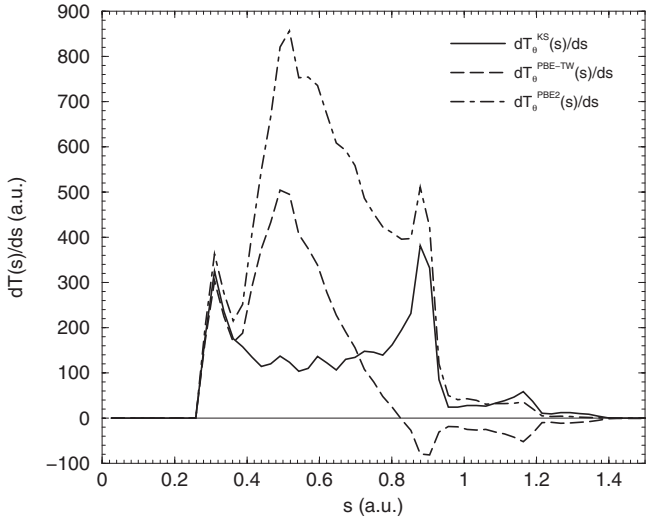

FIG. 1. Energy density contributions to the Pauli term T_θ as a function of s presented as values of $dT_\theta(s)/ds$ from Eq. (33); shown are conventional Kohn-Sham $dT_\theta^{\mathrm{KS}}(s)/ds$ (the reference), our PBE2 functional, and the older PBE-TW GGA functional. Data are for the SiO diatomic molecule at bond length 1.926 Å and are based on the density from fully numerical KS-LDA computations.

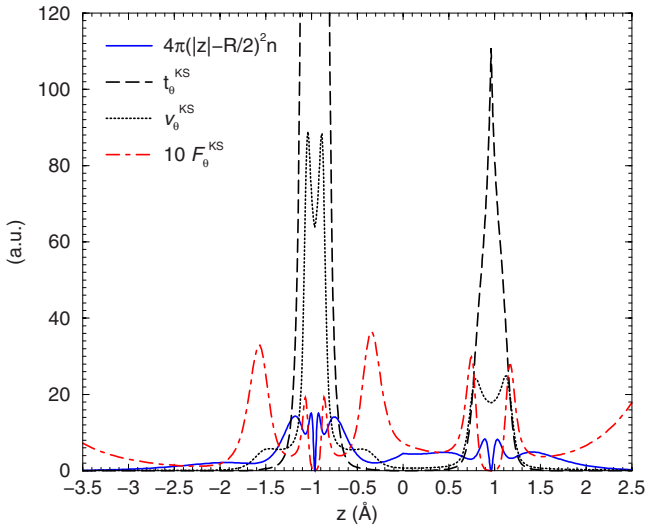

FIG. 2. (Color online) Conventional (reference) KS values for electronic density (scaled by the factor $4\pi(|z|-R/2)^2$, with R the internuclear distance), Pauli term t_θ, Pauli potential v_θ, and enhancement factor F_θ, calculated for points on the internuclear axis using KS-LDA fully numerical orbitals for the SiO molecule; Si at $(0,0,-0.963)$ Å, O at $(0,0,+0.963)$ Å.

ventional GGA PBE-TW functional has a spurious minimum at this point. Moreover, the PBE-TW Pauli term goes negative for all $s>0.82$. In addition, Fig. 1 shows that the KS kinetic energy is nearly totally determined by the behavior of F_θ over a relatively small range of s, approximately $0.26\leq s\leq 1.30$ for the SiO diatomic. The asymptotic regions ($s\to 0$ and $s\to\infty$) do not play a significant role. The range $0.26\leq s\leq 0.9$ has the highest weight of contribution (the highest differential contribution). As an aside, we surmise that PBE2 overestimates the KE because it was fitted purely to forces without regard to total energies.

Figures 2–4 provide comparisons of the reference t_θ^{KS}, v_θ^{KS}, and F_θ^{KS} (where $F_\theta^{\mathrm{KS}}\equiv t_\theta^{\mathrm{KS}}/c_0 n^{5/3}$) with the corresponding quantities for the PBE-TW and PBE2 approximations. The values are along the internuclear axis of the SiO molecule with internuclear separation 1.926 Å. The KS Pauli potential was calculated using the exact orbital-dependent expression

$$v_\theta([n];\mathbf{r}) = \frac{t_\theta([n];\mathbf{r})}{n(\mathbf{r})} + \sum_{i=1}^{N}(\varepsilon_N-\varepsilon_i)\frac{|\phi_i(\mathbf{r})|^2}{n(\mathbf{r})}, \qquad (35)$$

where ϕ_i and ε_i are the occupied KS orbitals and eigenvalues, respectively. Equation (35) is obtained in a way similar to that used in Ref. 29; see Ref. 8.

In Fig. 2, all three KS quantities, t_θ^{KS}, v_θ^{KS}, and F_θ^{KS} are everywhere *non-negative*, as they must be. Observe that v_θ^{KS} is *finite* at the nuclei and has local maxima at positions close to the intershell minima of the electronic density.

In contrast, the energy density of the PBE-TW Pauli term and corresponding enhancement factor have negative peaks in the intershell regions, violations of the non-negativity constraint for t_θ. However, addition to $t_\theta^{\mathrm{approx}}$ of any multiple of a Laplacian term $\nabla^2 n$ would change only the local behavior without altering the value of $T_\theta^{\mathrm{approx}}$, so the PBE-TW misbehavior might be resolved by such an addition. See discussion below. Figure 3 also shows that v_θ for the PBE-TW functional has very sharp negative peaks exactly at the nuclear positions in accord with Eq. (29).

Figure 4 shows that the modified-conjoint PBE2 v_θ respects the positivity constraint everywhere. Internuclear forces in the attractive region are described at least qualitatively correctly as a result. The PBE2 potential is still divergent at the nuclei in accordance with Eq. (29).

There are two small computational side issues. First, the absence of nuclear-site singularities in the computed correct Pauli potentials v_θ^{KS} might be argued to occur because the computed density does not have precisely the proper nuclear-site cusp, i.e., does not strictly obey Eq. (26). However, our numerical results are consistent with those in Ref. 27. Those authors used numerical orbitals[52] which presumably satisfied the cusp condition approximately. More importantly, if a specific numerical technique gives a KS density and associated KS t_s that produce a nonsingular v_θ, then an approximate v_θ evaluated with the *same* density should not introduce singularities. Second, the reader may notice that Fig. 4 shows small negative values for t_θ far from the bonding region of the molecule. This behavior seems to arise from numerical instability associated with fitting for small values of the density. In any event, those negative values make no appreciable contribution to the kinetic energy.

Finally, an insight to the harm of excess positivity of v_θ can be seen by examining the dependence of $T_\theta[n]$ upon v_θ. From a known virial relation[29] we have

$$T_\theta[n] = \frac{1}{2}\int v_\theta([n];\mathbf{r})(3+\mathbf{r}\cdot\nabla)n(\mathbf{r})d^3\mathbf{r}. \qquad (36)$$

Any spurious singularities of $v_\theta^{\mathrm{approx}}$ at the nuclei clearly will cause special problems in overweighting the integrand.

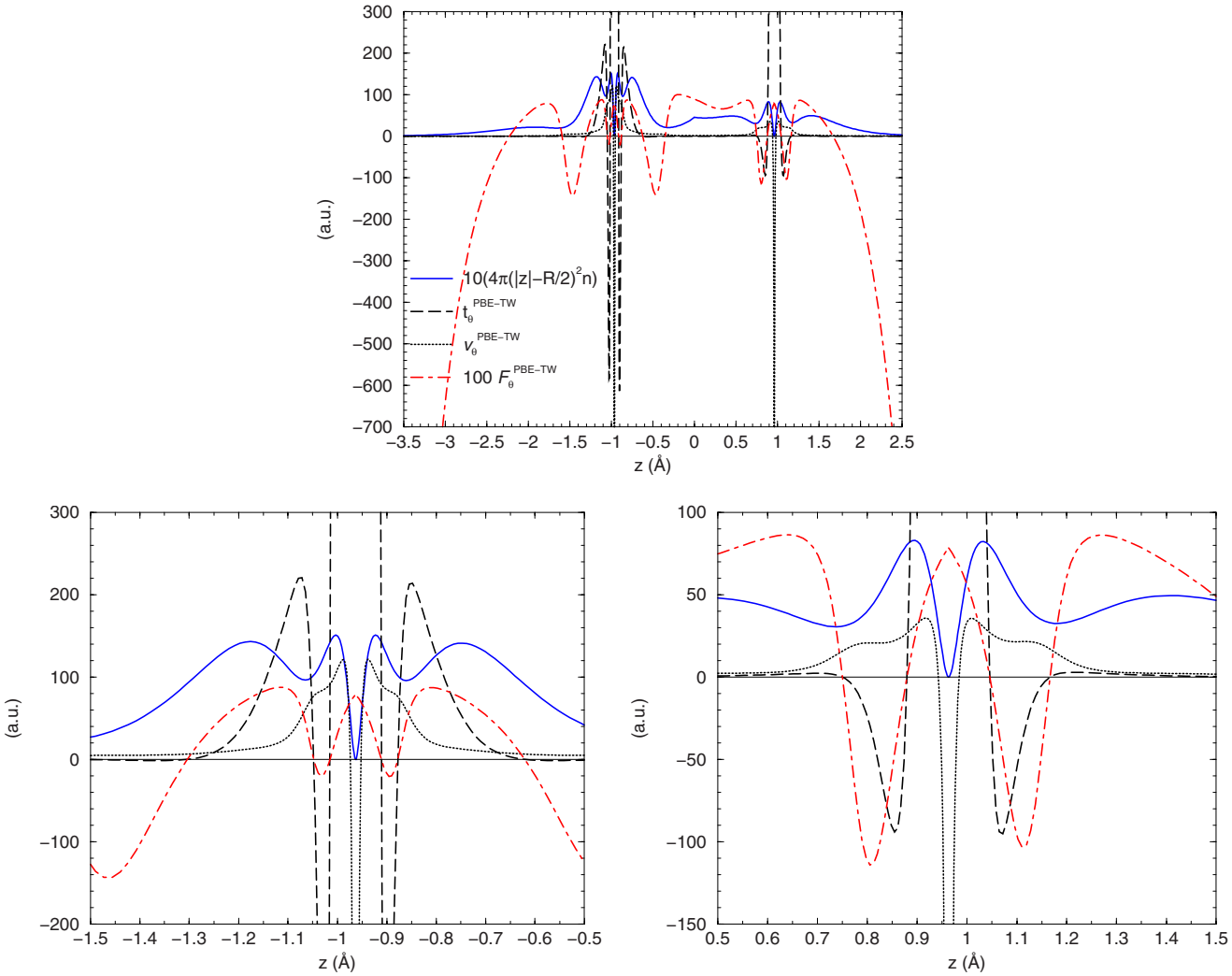

FIG. 3. (Color online) As in Fig. 2 for the PBE-TW conjoint approximation. Lower left panel: region near Si center; lower right panel: region near O center.

IV. BEYOND GGA-TYPE FUNCTIONALS

The preceding analysis makes clear the need for more flexible functionals than the forms of Eq. (30). In particular, nuclear-site divergences of v_θ are unavoidable for all purely GGA-type functionals, e.g., GGA, GGA-conjoint, and modified-conjoint KE functionals; recall Eqs. (28) and (29). Additional variables and constraints upon them are required to eliminate the singularities.

A. Reduced derivatives of the density

Consider again the gradient expansion of $T_s[n]$, Eq. (18) (see Refs. 35 and 53–55 for details), recast as

$$T_s[n] = \int \{t_0([n];\mathbf{r}) + t_2([n];\mathbf{r}) + t_4([n];\mathbf{r}) + \cdots\} d^3\mathbf{r}. \tag{37}$$

Here t_0 is as in Eq. (6), $t_2 = (1/9)t_W$, and

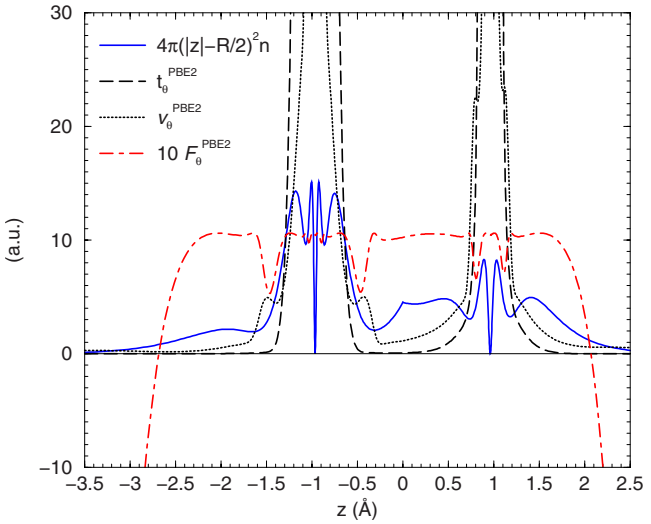

FIG. 4. (Color online) As in Fig. 2 for the PBE2 modified-conjoint approximation.

$$t_4([n];\mathbf{r}) = \frac{1}{540(3\pi^2)^{2/3}} n^{5/3}(\mathbf{r}) \left[\left(\frac{\nabla^2 n(\mathbf{r})}{n^{5/3}(\mathbf{r})} \right)^2 - \frac{9}{8} \left(\frac{\nabla n(\mathbf{r})}{n^{4/3}(\mathbf{r})} \right)^2 \left(\frac{\nabla^2 n(\mathbf{r})}{n^{5/3}(\mathbf{r})} \right) + \frac{1}{3} \left(\frac{\nabla n(\mathbf{r})}{n^{4/3}(\mathbf{r})} \right)^4 \right]. \tag{38}$$

The sixth-order term, dependent upon n, $|\nabla n|$, $\nabla^2 n$, $|\nabla \nabla^2 n|$, and $\nabla^4 n$, is given in Ref. 53.

Once again, in a finite system (e.g., molecule), a Laplacian-dependent term $\nabla^2 n$ affects only the local behavior of the kinetic energy density. Arguments have been advanced for and against including such Laplacian dependence in the KE density functional; for example, see Refs. 24, 51, 55, and 56. Recently Perdew and Constantin[19] presented a KE functional that depends on $\nabla^2 n$ via a modified fourth-order gradient expansion. Though not stated as such, their functional obeys the decomposition of Eq. (7). It is intended to be universal (or at least very broadly applicable), whereas we are focused on simpler functionals that may require parametrization to families of systems. The Perdew-Constantin form involves a rather complicated functional interpolation between the gradient expansion and the von Weizsäcker functional. They did not discuss the corresponding potential v_θ nor Born-Oppenheimer forces and they characterized the performance of their functional for the energetics of small molecule dissociation as "still not accurate enough for chemical applications." So we proceed rather differently.

Rearrange the foregoing gradient expansion into $T_W + T_\theta$ form [recall Eq. (7)]:

$$\begin{aligned} T_\theta[n] &= \int \left[c_0 n^{5/3}(\mathbf{r}) \left(1 - \frac{40}{27} s^2 \right) + t_4 + t_6 + \cdots \right] d^3\mathbf{r} \\ &= \int \left[t_0 \left(1 - \frac{5}{3} s^2 \right) + t_0 \frac{5}{27} s^2 + t_4 + t_6 + \cdots \right] d^3\mathbf{r} \\ &\equiv \int [t_\theta^{(0)}([n];\mathbf{r}) + t_\theta^{(2)}([n];\mathbf{r}) + t_\theta^{(4)}([n];\mathbf{r}) + \cdots] d^3\mathbf{r}, \end{aligned} \tag{39}$$

where

$$t_\theta^{(0)}([n];\mathbf{r}) = t_0([n];\mathbf{r}) \left[1 - \frac{5}{3} s^2 \right], \tag{40}$$

$$t_\theta^{(2)}([n];\mathbf{r}) = t_0([n];\mathbf{r}) \left[\frac{5}{27} s^2 \right], \tag{41}$$

and

$$t_\theta^{(4)}([n];\mathbf{r}) = t_0([n];\mathbf{r}) \left[\frac{8}{81} \left(p^2 - \frac{9}{8} s^2 p + \frac{1}{3} s^4 \right) \right]. \tag{42}$$

Each term, Eqs. (40)–(42), of Eq. (39) can be put straightforwardly into a GGA-like form:

$$t_\theta^{(2i)}([n];\mathbf{r}) = t_0([n];\mathbf{r}) F_\theta^{(2i)}(s,p,\ldots), \tag{43}$$

where s, p are as in Eqs. (11) and (23), respectively. The first two terms of the expansion yield the SGA enhancement factor already discussed,

$$F_\theta^{\mathrm{SGA}} \equiv F_\theta^{(0)} + F_\theta^{(2)} = 1 + a_2 s^2, \tag{44}$$

with $a_2 = -40/27$. The fourth-order (in highest power of s) term is

$$F_\theta^{(4)} = a_4 s^4 + b_2 p^2 + c_{21} s^2 p, \tag{45}$$

with coefficients $a_4 = 8/243$, $b_2 = 8/81$, and $c_{21} = -1/9$.

Rather than retain those values of a_2, a_4, b_2, and c_{21}, we instead treat them as parameters and seek values or relationships among them which would yield a nonsingular v_θ through a given order. (Corresponding improvement of Thomas-Fermi theory by imposition of the nuclear cusp condition was introduced in Ref. 57.)

Functional differentiation of each term in Eq. (39) gives the formal gradient expansion $v_\theta = v_\theta^{(0)} + v_\theta^{(2)} + v_\theta^{(4)} + \cdots$, where $F_\theta^{(2i)}$ (shown below with its arguments suppressed for clarity) is a function of s^2, p, and in principle, higher derivatives of $n(\mathbf{r})$:

$$\begin{aligned} v_\theta^{(2i)}(\mathbf{r}) = t_0([n];\mathbf{r}) & \times \left[\frac{5}{3n(\mathbf{r})} F_\theta^{(2i)} + \frac{\partial F_\theta^{(2i)}}{\partial (s^2)} \frac{\partial (s^2)}{\partial n(\mathbf{r})} + \frac{\partial F_\theta^{(2i)}}{\partial p} \frac{\partial p}{\partial n(\mathbf{r})} + \cdots \right] \\ & - \nabla \cdot \left[t_0([n];\mathbf{r}) \frac{\partial F_\theta^{(2i)}}{\partial (s^2)} \frac{\partial (s^2)}{\partial \nabla n(\mathbf{r})} \right] \\ & + \nabla^2 \left[t_0([n];\mathbf{r}) \frac{\partial F_\theta^{(2i)}}{\partial p} \frac{\partial p}{\partial \nabla^2 n(\mathbf{r})} \right] + \cdots. \end{aligned} \tag{46}$$

The ellipses in Eq. (46) correspond to additional terms that are needed only if $F_\theta^{(2i)}$ depends upon derivatives other than s and p.

After manipulation (see Appendix A), one obtains the potentials corresponding to the enhancement factors in Eqs. (44) and (45):

$$v_\theta^{\mathrm{SGA}} = c_0 n^{2/3} \left[\frac{5}{3} + a_2 s^2 - 2 a_2 p \right], \tag{47}$$

$$\begin{aligned} v_\theta^{(4)} = c_0 n^{2/3} \Bigg[& \left(11 a_4 + \frac{88}{9} c_{21} \right) s^4 - (5 b_2 + 2 c_{21}) p^2 \\ & - \left(4 a_4 - \frac{80}{9} b_2 \right) s^2 p - \left(8 a_4 + \frac{32}{3} c_{21} \right) q - \frac{20}{3} b_2 q' \\ & + 2 b_2 q'' + 2 c_{21} q''' \Bigg]. \end{aligned} \tag{48}$$

Here q is as in Eq. (24) and q', q'', and q''' are other dimensionless fourth-order reduced density derivatives defined as

$$q' \equiv \frac{\nabla n \cdot \nabla \nabla^2 n}{(2k_F)^4 n^2} = \frac{\nabla n \cdot \nabla \nabla^2 n}{16(3\pi^2)^{4/3} n^{10/3}}, \tag{49}$$

$$q'' \equiv \frac{\nabla^4 n}{(2k_F)^4 n} = \frac{\nabla^4 n}{16(3\pi^2)^{4/3} n^{7/3}}, \tag{50}$$

$$q''' \equiv \frac{\nabla\nabla n:\nabla\nabla n}{(2k_F)^4 n^2} = \frac{\nabla\nabla n:\nabla\nabla n}{16(3\pi^2)^{4/3} n^{10/3}}. \tag{51}$$

The operation denoted by the colon in the numerators of q''' is $A:B \equiv \Sigma_{ij} A_{ij} B_{ji}$.

At Eq. (28) we have already pointed out that an enhancement factor of SGA form, specifically, that of Eq. (44), produces a Pauli potential

$$v_\theta^{\mathrm{SGA}}(r) = v_\theta^{(0)}(r) + v_\theta^{(2)}(r) = \frac{3}{5}\frac{Za_2}{r} + \text{nonsingular terms}. \tag{52}$$

This exhibits the $1/r$ SGA Pauli potential nuclear singularity already discussed; we return to this point in a moment.

For the fourth-order enhancement factor, Eq. (45), we again note that s and q are nonsingular near the nucleus, while

$$\lim_{r\to 0} s^2(r) = Z^2/[3\pi^2 n(0)]^{2/3}. \tag{53}$$

With a density of the form of Eq. (27), Eq. (48) thus gives the near-nucleus behavior of the fourth-order potential as

$$v_\theta^{(4)}(r) = \frac{c_0}{16[9\pi^4 n(r)]^{2/3}}\left[-\frac{16Z^2}{3r^2}(5b_2+3c_{21}) + \frac{32Z^3}{9r}(18a_4 + 17b_2 + 18c_{21})\right] + \text{nonsingular terms}. \tag{54}$$

The singularities in $1/r^2$ and $1/r$ can be removed by requiring that the numerators of the first two terms of Eq. (54) both vanish. This is equivalent to imposition of constraints on the coefficients, namely,

$$c_{21} = -\frac{5}{3}b_2,$$

$$a_4 = \frac{13}{18}b_2. \tag{55}$$

In the spirit of the GGA, we are led to defining a fourth-order reduced density derivative (RDD) as

$$\kappa_4 = s^4 + \frac{18}{13}p^2 - \frac{30}{13}s^2 p. \tag{56}$$

This RDD with Eq. (45) gives an enhancement factor

$$F_\theta^{(4)}(\kappa_4) = a_4\kappa_4, \tag{57}$$

which yields a Pauli potential with *finite* values at point nuclei. Clearly it is not the only κ_4-dependent enhancement factor with that property. So, we seek $F_\theta^{(4)}(\kappa_4)$ functional forms which are more general than Eq. (57) and which give a positive-definite nonsingular v_θ. A few examples were given in Ref. 8.

At this point, it is prudent to consider how many terms in the Taylor series expansion of the density Eq. (27) are relevant for the cancellation of singularities in Eq. (54). The answer is four terms: $n(r) \propto 1 - 2Zr + 2Z^2r^2 - (4/3)Z^3r^3$. That is, the singularities will reappear for a density of the form of Eq. (26) if the second- and third-order terms differ from those defined by a hydrogenlike density expansion, e.g., Eq. (27). Thus, the foregoing cancellation fails for a density with power series expansion $n(r) \propto 1 - 2Zr - (4/3)Z^3r^3 + \cdots$. This fact will limit applications of simple κ_4-based KE functionals to those densities which have precisely hydrogenlike behavior up to fourth order.

It is necessary, therefore, to consider other candidates for RDD variables which would provide cancellation of singularities for the density Eq. (26) independently of hydrogenic higher-order terms in the Taylor series expansion of the density. The observation that $\kappa_4 \sim O(\nabla^4)$ suggests that the effective or operational order of ∇ in such a candidate variable should be reduced to second order. This in turn suggests a candidate variable, still based on the fourth-order gradient expansion Eq. (42), namely,

$$F_\theta^{(4-2)} = \sqrt{a_4 s^4 + b_2 p^2 + c_{21} s^2 p} \tag{58}$$

[compare Eq. (45)]. Now consider a density of the form of Eq. (26) but with arbitrary first- and higher-order near-nucleus expansion coefficients,

$$n(r) \sim (1 + C_1 r + C_2 r^2 + C_3 r^3). \tag{59}$$

Following the same lines as those used to reach Eq. (54), one finds

$$v_\theta^{(4-2)}(r) \sim \frac{c_{21}}{\sqrt{b_2}}\frac{1}{r} + \text{nonsingular terms}. \tag{60}$$

The singular term would be eliminated by the choice $c_{21}=0$. The cancellation is universal in that it does not depend on the density expansion coefficients, C_i (while the singular term prefactor and nonsingular terms do, of course, depend on those expansion coefficients). Hence a candidate RDD variable (denoted as $\tilde{\kappa}_4$) which provides cancellation of singular terms in the Pauli potential could be defined as

$$\tilde{\kappa}_4 = \sqrt{s^4 + b_2 p^2}, \quad b_2 > 0. \tag{61}$$

Note that this form is manifestly positive.

This RDD can be used to construct a variety of enhancement factors to replace Eq. (45) for the fourth-order approximation to the Pauli term, for example, $F_\theta(\tilde{\kappa}_4) = a_4\tilde{\kappa}_4$. This simplest enhancement factor corresponds to a Pauli potential with *finite* values at point nuclei but clearly it is not the only $\tilde{\kappa}_4$-dependent one with that property. Any linear combination of nonsingular enhancement factors (including the simple $F_\theta = 1$) also will be nonsingular. A combination of two PBE-like forms [see Eq. (71) below] is also nonsingular, as can be checked analytically for any density with near-nucleus behavior defined by Eq. (59), hence, also Eqs. (26) and (27).

There are, of course, $\tilde{\kappa}_4$-dependent functionals that yield a divergent potential, e.g.,

$$F_\theta(\tilde{\kappa}_4) = \tilde{\kappa}_4^2 \tag{62}$$

so one must be cautious.

Regarding the second-order forms, Eq. (52) shows that, short of complete removal of the s^2 term from F_θ^{SGA}, we cannot cure the singularity in v_θ^{SGA}. There is no direct analogy to the removal of singularities in $v_\theta^{(4)}$ just discussed. Instead, in parallel with Eq. (56) or Eq. (61), we introduce a second-order RDD,

$$\kappa_2 = s^2 + b_1 p, \tag{63}$$

with b_1 to be determined. Then, in analogy with a PBE-type enhancement factor, we can define an enhancement factor dependent only on second-order variables as

$$F_\theta^{(2)}(\kappa_2) = \frac{\kappa_2}{1+\alpha\kappa_2}. \tag{64}$$

For it, the near-nucleus (small r) behavior of the Pauli potential is

$$v_\theta^{(2)}(r) = C_1^{(2)}\frac{(1+C_2^{(2)}b_1\alpha)}{b_1\alpha^2} + O(r), \tag{65}$$

with constants $C_i^{(2)} > 0$ which depend on the specific density behavior being handled.

The RDDs considered thus far are combinations of powers of s and p which ensure cancellation of nuclear cusp divergences in v_θ. Thus, we define a class of approximate KE functionals, the reduced derivative approximation (RDA) functionals, as those with enhancement factors depending on the RDDs,

$$T_{\mathrm{s}}^{\mathrm{RDA}}[n] \equiv T_{\mathrm{W}}[n] + \int t_0([n];\mathbf{r})F_\theta(\kappa_2(\mathbf{r}),\tilde{\kappa}_4(\mathbf{r}))d^3\mathbf{r}, \tag{66}$$

[$t_0[n]$ from Eq. (6)] with nondivergent Pauli potentials as a consequence of constraints imposed on the coefficients in the RDDs. This route of development of KE functionals is under active investigation; see below.

For insight, Fig. 5 shows the behavior of the RDD $\tilde{\kappa}_4$ along the SiO internuclear axis for four values of b_2. The behavior in the vicinity of the Si atom is shown. Both the s and p variables have four maxima which lie close to the intershell minima in the density. Increasing the value of b_2 increases the height of the corresponding maxima for $\tilde{\kappa}_4$ RDD (because the contributions from the p maxima increase). Behavior of the RDD κ_2 is defined by a linear combination of the s and p variables.

One of the peculiarities is that the reduced density Laplacian p is divergent at the nucleus and, as a consequence, κ_2 and $\tilde{\kappa}_4$ itself also are divergent, even though it generates a nondivergent v_θ. This divergence will not affect the KE enhancement factors provided that $\lim_{\kappa_2\to\infty} F_\theta(\kappa_2) = \text{constant}$ and $\lim_{\tilde{\kappa}_4\to\infty} F_\theta(\tilde{\kappa}_4) = \text{constant}$. One of the advantages of the $\tilde{\kappa}_4$ variable is its positiveness everywhere (by definition).

Consider near-nucleus behavior in a bit more detail. In that region, the electron-nuclear cusp condition[38–42] means that the density will have hydrogenic form (at least to first order); recall Eq. (27). For such an N-electron density, one can form N orthonormal isodensity orbitals,[58]

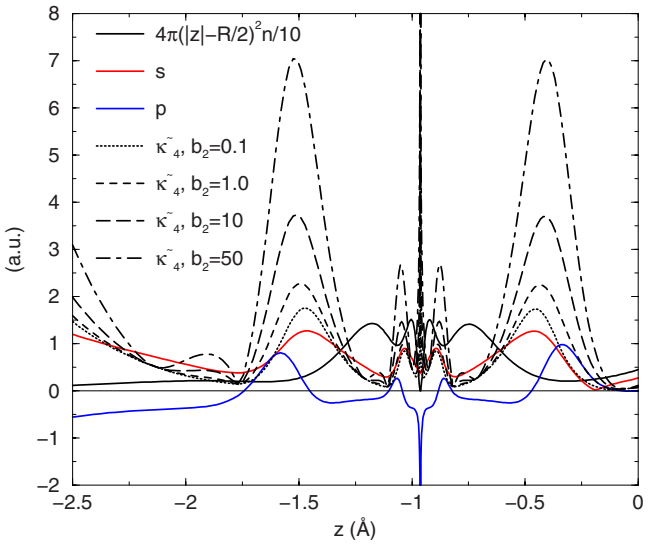

FIG. 5. (Color online) The fourth-order $\tilde{\kappa}_4$ reduced density derivative for different values of b_2 along the internuclear axis z for the SiO diatomic molecule near the Si atom: Si at (0,0,−0.963) Å; O at (0,0,+0.963) Å. Variables s and p are shown for comparison.

$$\chi_m(\mathbf{r}) = \frac{A_m}{N^{1/2}} n^{1/2}(\mathbf{r}) \exp i g_m(\mathbf{r}). \tag{67}$$

Orthogonality of the χ_m requires

$$N^{-1}A_m A_n \int d\mathbf{r} n(\mathbf{r}) \exp i[g_m(\mathbf{r}) - g_n(\mathbf{r})] = \delta_{m,n}. \tag{68}$$

For $n(\mathbf{r})$ of the form Eq. (27), the orthogonal functions $\exp ig_m(\mathbf{r})$ have an exponential weight factor, hence, must be proportional to the generalized Laguerre polynomials of degree 2 (from the Jacobian r^2) multiplied by suitable spherical harmonics. See, for example, Ref. 59. While in principle one could make any arbitrary unitary transformation (but not local gauge transformation) of these N isodensity orbitals, that would not change the KE. So we can put aside such a transformation. Then, in the limit that one approaches the nucleus, the dominant orbital is the $\ell=0$ which is either singly or doubly occupied; hence, the KE density is arbitrarily close to t_{W} in that region. Therefore T_θ is arbitrarily close to zero in that same region. A sufficient condition for this behavior is that F_θ also be arbitrarily close to zero in that region. For T_θ^{KS} this is essentially what happens, as shown in Fig. 6. It gives a blown-up view of the region around the oxygen nucleus for the SiO molecule shown in Fig. 2. At the nucleus, $F_\theta^{\mathrm{KS}} \approx 0.004$. Thus, in that region $F_t \approx F_{\mathrm{W}}$. Numerically, for the systems we have tested, we find $s \approx 0.37 \to 0.38$ in that region, so we expect

$$F_t(r\to 0) = F_{\mathrm{W}}(r\to 0) = \frac{5}{3}s^2(r\to 0) \approx 0.23. \tag{69}$$

Asymptotically, the density of an isolated system decays to zero exponentially and the inhomogeneity variable diverges: $s\to\infty$ as $r\to\infty$. Because of this asymptotic hydrogenic character, it is generally supposed that the von

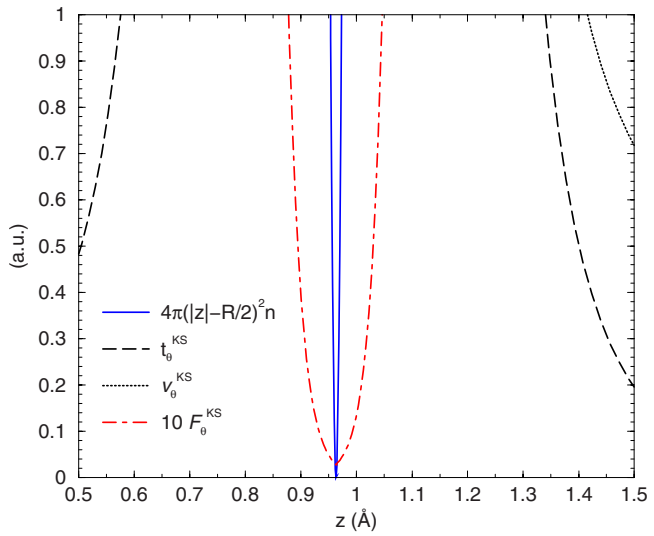

FIG. 6. (Color online) Blow-up of data from Fig. 2 for the region immediately around the O atom. Notation the same.

Weizsäcker functional again is a reasonable approximation.[11] This behavior is the case for systems for which the tail region has the one-particle reduced density matrix dominated by a single valence orbital $\gamma(\mathbf{r},\mathbf{r}')=f_i\psi_i(\mathbf{r})\psi_i^*(\mathbf{r}')$ occupied by one or two electrons. But that is not the case for all systems at large but finite distances. For example, numerical calculations for the SiO molecule show that two valence orbitals, 7σ and 6σ, have similar magnitude in the tail region (see Fig. 7). As a consequence $\gamma(\mathbf{r},\mathbf{r}')=2\psi_{6\sigma}(\mathbf{r})\psi_{6\sigma}^*(\mathbf{r}')+2\psi_{7\sigma}(\mathbf{r})\psi_{7\sigma}^*(\mathbf{r}')$ in the tail region (at least near the internuclear axis). Hence, the von Weizsäcker KE functional is not an appropriate approximation in the large but finite-distance part of the tail region of that molecule. The Pauli term enhancement factor, in fact, is not small there, but has growing values (recall Fig. 2).

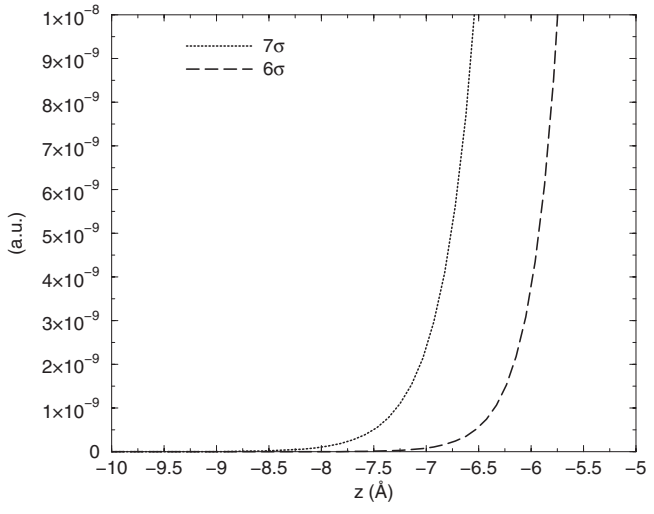

FIG. 7. Fully numerical KS-LDA valence orbitals $|\psi_{7\sigma}|^2$ and $|\psi_{6\sigma}|^2$ for the SiO molecule calculated for points on the internuclear axis in the tail region.

B. Parametrization of a RDA functional

In addition to the positive singularities, another limitation of our earlier modified-conjoint-type KE functionals was the inability to parametrize them to provide both forces and total energies simultaneously.[7] Given the emphasis on MD simulations, parametrization to the forces was the priority. With the spurious repulsive singularities removed from RDD functionals, the question arises whether total energy parametrization can be used and, if so, if it is beneficial. The usual *energy* fitting criterion is to minimize

$$\omega_E=\sum_{i=1}^{m}|E_i^{\mathrm{KS}}-E_i^{\text{OF-DFT}}|^2 \tag{70}$$

over systems (e.g., atoms and molecules) and configurations (e.g., diatomic molecule bond length) indexed generically here by i. When the parameter adjustment is done for fixed-density inputs (i.e., conventional KS densities as inputs), this total energy optimization is equivalent to optimization of the T_s functional. We did this for determination of the empirical parameters for the new RDA-type functionals $F_\theta^{\mathrm{RDA}}=F_\theta(\kappa_2,\tilde{\kappa}_4)$.

Since $F_\theta=1$ (or any constant in general) also yields a nonsingular Pauli potential, we can form κ_2, $\tilde{\kappa}_4$-dependent enhancement factors which resemble GGA forms and thereby enable connection with the modified-conjoint GGA functionals discussed already. One form which we have begun exploring (see below) is

$$F_\theta^{m0}(\{\kappa\})=A_0+A_1\left(\frac{\tilde{\kappa}_{4a}}{1+\beta_1\tilde{\kappa}_{4a}}\right)^i+A_2\left(\frac{\tilde{\kappa}_{4b}}{1+\beta_2\tilde{\kappa}_{4b}}\right)^j+A_3\left(\frac{\kappa_{2c}}{1+\beta_3\kappa_{2c}}\right)^k. \tag{71}$$

A_i and β_i are parameters to be determined, along with the constants a, b, and c which appear in the definition of the $\tilde{\kappa}_4$ and κ_2 variables; see Eqs. (61) and (63). Even this simple form has two desirable properties: (i) the corresponding v_θ is finite for densities with the near-nucleus behavior defined by Eq. (59), hence, also Eq. (26) or Eq. (27) (this has been checked by explicit analytical calculation); (ii) the divergences of $\tilde{\kappa}_{4a}$, $\tilde{\kappa}_{4b}$, and κ_2 near the nucleus (see Fig. 5) cancel in Eq. (71) ($\lim_{\{\tilde{\kappa}_{4a},\tilde{\kappa}_{4a},\kappa_{2c}\}\to\infty}F_\theta^{m0}(\{\kappa\})=A_0+A_1/\beta_1^i+A_2/\beta_2^j+A_3/\beta_3^k$). Positivity of F_θ^{m0} depends on the specific parameters of the functional, hence, must be checked for each case.

After limited exploration, we used $i=2$, $j=4$, and $k=1$. Again because the motivating materials problem was brittle fracture in the presence of water, our choice of training set M has a focus on Si and O. In an attempt to gain a bit of generality, we used two molecules with Si-O bonds and two closed shell atoms $M=\{H_6Si_2O_7,H_4SiO_4,\mathrm{Be},\mathrm{Ne}\}$, with a set of six bond lengths for each molecule. In detail, for the $H_6Si_2O_7$ one of the central Si-O bond lengths was varied: $R(\mathrm{Si}_1\text{-}\mathrm{O}_1)=\{1.21,1.41,1.61,1.91,2.21,2.81\}$ Å. For H_4SiO_4, the deformation was in T_d mode, that is, all four Si-O bonds were changed identically: $R(\mathrm{Si}\text{-}\mathrm{O}_i)=\{1.237,1.437,1.637,1.937,2.237,2.437\}$ Å. KS-LDA den-

TABLE I. KS kinetic energy T_s values (in hartrees) for the first ten atoms and differences ($T_s^{\text{OF-DFT}} - T_s^{\text{KS}}$) calculated using a GGA (Thakkar), MGGA, and RDA explicit semilocal approximate functionals. LDA-KS densities for LDA equilibrium geometries (calculated as described in Appendix B) were used as input.

	KS	Thakkar	MGGA	RDA
H	0.469	0.009	0.019	0.019
He	2.774	−0.002	0.177	0.008
Li	7.250	0.041	0.257	0.180
Be	14.328	0.045	0.284	0.197
B	24.180	0.022	0.112	0.231
C	37.249	−0.005	0.186	0.276
N	53.966	0.140	0.393	0.282
O	74.177	−0.174	−0.013	0.189
F	98.670	−0.385	0.142	0.094
Ne	127.700	−0.237	0.567	−0.006
MAE[a]		0.106	0.215	0.148

[a]MAE=mean absolute error.

sities and energies were the inputs (again see Appendix B for computational details). Minimization of the target function defined by Eq. (70) gave $A_0=0.506\,16$, $A_1=3.041\,21$, $A_2=-0.345\,67$, $A_3=-1.897\,38$, $\beta_1=1.296\,91$, $\beta_2=0.561\,84$, $\beta_3=0.219\,44$, and $a=46.476\,62$, $b=18.806\,58$, and $c=-0.903\,46$.

The KE functional defined by Eq. (71) does not satisfy several of the exact constraints. A simple check shows that $F_\theta^{m0}(\{\kappa_2,\tilde{\kappa}_4\})$ unfortunately is not positive for all values of κ_2 and for all positive values of $\tilde{\kappa}_4$ (recall that $\tilde{\kappa}_4$ is positive by definition). Moreover, it does not recover the constant density limit nor is its F_θ contribution to F_t small at the nucleus (recall discussion at the end of preceding section). These deficiencies illustrate the challenge in finding the universal functional. A pressing question is which constraints should be placed at higher priority than others when using a functional form as simple as defined by Eq. (71). One part of exploring that issue is to study how well or poorly this functional does despite the constraint violations.

Table I shows kinetic energies for the first row atoms from conventional KS calculations and from approximate OF-DFT functionals using the KS density as input. The Thakkar empirical functional[50] was chosen as an example of a GGA KE functional. The Perdew-Constantin meta-GGA (Ref. 19) "MGGA" was chosen because it, like our functional, is based on quantities that are at fourth order in the density gradient expansion. The mean absolute errors (MAE) for the GGA and RDA-*m*0 functionals are of the same order of magnitude, with the distinction that the GGA functional underestimates the KE for the He, C, O, and F atoms, whereas RDA-*m*0 overestimates. The underestimates may be a sign of violation of *N* representability. We defer discussion of that issue to Sec. V. The MAE for the MGGA functional is 50% larger than for RDA-*m*0 and 100% for GGA.

Table II displays kinetic energies for 14 molecules (four of them with Si-O bonds) calculated at equilibrium geometries with the conventional KS method and with the same

TABLE II. KS kinetic energy T_s values (in hartrees) for selected molecules and differences ($T_s^{\text{OF-DFT}} - T_s^{\text{KS}}$) calculated using a GGA (Thakkar), MGGA, and RDA explicit semilocal approximate functionals. LDA-KS densities for LDA equilibrium geometries (calculated as described in Appendix B) were used as input.

	KS	Thakkar	MGGA	RDA
H_2	1.080	−0.022	0.103	0.036
LiH	7.784	0.021	0.296	0.161
H_2O	75.502	−0.285	0.318	−0.188
HF	99.390	−0.353	0.329	−0.171
N_2	108.062	−0.340	0.300	−0.182
LiF	106.183	−0.261	0.566	0.175
CO	111.832	−0.333	0.300	−0.179
BF	123.117	−0.273	0.456	0.080
NaF	260.097	−0.348	1.295	0.711
SiH_4	290.282	0.084	3.112	0.574
SiO	362.441	−0.262	2.825	0.370
H_4SiO	364.672	−0.163	3.338	0.421
H_4SiO_4	587.801	−0.860	4.133	−0.081
$H_6Si_2O_7$	1100.227	−1.408	7.968	0.064
MAE[a]		0.358	1.810	0.242

[a]MAE=mean absolute error.

three approximate OF-DFT functionals (Thakkar-GGA, MGGA, and RDA), again using the KS density as input for the approximate functional calculations. The results are a bit surprising, because the MAE for the RDA-*m*0 functional is about 2/3 the MAE for the GGA KE and less than 1/7 the MAE for the MGGA. Given that the GGA is heavily parametrized compared to the small RDA-*m*0 training set (recall *M* above; two molecules with Si-O bonds and two closed shell atoms), we had not expected to obtain such comparatively good transferability to other systems.

Because the objective is a KE functional capable of predicting correct interatomic forces, an important aspect of any functional is its behavior in the attractive regions of the potential surface. Table III shows energy gradients for the molecules listed in Table II calculated at the stretched bond length(s) for which the "exact" (i.e., reference) KS attractive force has maximum magnitude. One and two bonds were deformed in the water molecule [respectively denoted in the table as $H_2O(1R)$ and $H_2O(2R)$], while SiH_4 and H_4SiO_4 were deformed in T_d mode, and only one Si-O bond was stretched in H_4SiO and $H_6Si_2O_7$.

The forces were calculated by a three-point centered finite-difference formula. As found previously and summarized above, the GGA functionals (again the Thakkar functional is the GGA example) generally are incapable of predicting the correct sign (attraction) for the force. The only molecules in Table III for which GGA predicts attraction are H_2, LiH, and SiH_4. The MGGA functional behaves rather similarly, with its predicted energy gradient having the wrong sign in most cases. In contrast, for all of the table entries, the RDA-*m*0 functional predicts the correct sign of the gradient. In many cases [$H_2O(1R)$, $H_2O(2R)$, HF, CO, BF, H_4SiO, H_4SiO_4, and $H_6Si_2O_7$] it yields values very close to the reference KS results.

TABLE III. Energy gradient (hartree/Å) calculated at point R_m corresponding to the extremum of attractive force as calculated by the KS method. Approximate OF-DFT energy gradients are obtained by replacing T_s^{KS} by $T_s^{OF\text{-}DFT}$. LDA-KS densities for LDA equilibrium geometries (calculated as described in Appendix B) were used as input.

	R_m (Å)	KS	Thakkar	MGGA	RDA
H_2	1.2671	0.164	0.029	0.112	0.017
LiH	2.455	0.046	0.016	0.037	0.028
H_2O(1R)	1.3714	0.216	−0.050	−0.073	0.261
H_2O(2R)	1.3714	0.416	−0.127	−0.163	0.454
HF	1.3334	0.232	−0.071	−0.003	0.192
N_2	1.3986	0.576	−0.349	−0.819	0.212
LiF	2.0405	0.079	−0.019	−0.032	0.041
CO	1.4318	0.474	−0.248	−0.659	0.472
BF	1.6687	0.207	−0.037	−0.118	0.244
NaF	2.4284	0.067	−0.007	1.169	0.157
SiH_4	1.9974	0.447	0.102	0.189	0.088
SiO	1.9261	0.278	−0.098	−0.281	0.125
H_4SiO	2.057	0.162	−0.027	−0.086	0.113
H_4SiO_4	2.037	0.712	−0.278	−0.714	0.600
$H_6Si_2O_7$	2.010	0.194	−0.022	−0.173	0.117

Figure 8 shows the energy for the water molecule as a function of the O-H_1 bond length. Again, neither the GGA nor the MGGA curve exhibits a minimum. This is a case for which the new RDA-*m*0 functional behaves relatively poorly. Though it yields a minimum, it is at too large a bond length, while in the tail region the RDA-*m*0 curve goes almost flat. Thus, the structure predicted by RDA-*m*0 would be more expanded than the correct value and the attractive force in the tail region would be significantly underestimated. The "DPK-refitted" curve corresponds to the DePristo and Kress KE functional[49] with all seven parameters refitted using exactly the same fitting procedure as used for the RDA-*m*0 functional. The refitted DPK curve fails to yield a minimum not only for the water molecule (not included in the fitting set) but also for one of the molecules (H_4SiO_4) from the fitting set. For the other fitting set molecule ($H_6Si_2O_7$), the curve has unphysical behavior, namely, dual minima. From this comparison, one deduces that the comparative success of the RDA-*m*0 is not an artifact of the fitting procedure but instead is a consequence of using the new RDD variables which provide correct behavior of the Pauli potential in the region near the nucleus. Of course the correct behavior of the Pauli potential (non-negativeness, nonsingularity at nucleus) is not a sufficient condition for good performance of a KE functional.

Regarding the behavior of the MGGA, there is another interesting aspect of finding energy minima. Very recently Constantin and Ruzsinszky[60] have presented binding energies as a function of bond length for the N_2 molecule for various orbital-free KE functionals including both TF and MGGA. Both functionals *overbind* the molecule. Since TF cannot bind a molecule on fundamental grounds (Teller's theorem[25]), attention is drawn immediately to their procedure. It appears plausible that the reason for their contradictory outcome is the use of broken-symmetry Hartree-Fock densities as input. There simply is no guarantee that use of one of these functionals in the OF-DFT Euler equation, Eq. (4), would generate anything like the HF density. The contradictory outcome confirms that, in fact, the self-consistent OF-DFT density with one of these functionals would differ in crucial ways. Reference 60 does, however, raise two subtle and difficult issues, namely, that symmetry-broken solutions do occur and that it is not obvious how to get such solutions out of a full self-consistent OF-DFT treatment.

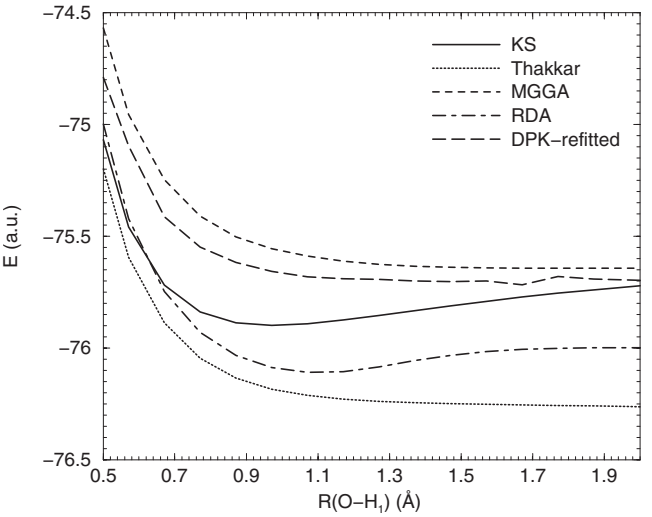

FIG. 8. Total energy as a function of the O-H_1 distance for the H_2O molecule (with O-H_2 kept at its equilibrium value) obtained from a KS calculation with LDA XC and from approximate GGA (Thakkar), MGGA (Perdew-Constantin), RDA-*m*0, and DPK-refitted functionals. Refitted parameters of the DPK-refitted functional are the following: $a_1=0.596\,85$, $a_2=16.623\,26$, $a_3=17.200\,09$, $a_4=3.676\,44$, $b_1=-0.840\,67\times10^{-2}$, $b_2=12.689\,84$, $b_3=-0.285\,64\times10^{-4}$. The LDA KS densities (calculated as described in Appendix B) were used as input to the orbital-free functionals.

C. Atomic analysis of the RDA-*m*0 functional

For further analysis of the RDA-*m*0 functional, we calculated the Pauli potential near the nucleus ($r\to0$) for the Be atom using a simple H-like model density. A single-ζ Slater orbital density with exponents $\zeta_{1s}=3.6848$ and $\zeta_{2s}=0.9560$ taken from Ref. 61 near $r=0$ has the following Taylor series expansion: $n(r)\approx415.0479\times(1-7.3971r)$. The density $n(r)=415.0479\times\exp(-7.3971r)$ has the same slope at $r=0$. It can be used as an approximate density for the Be atom near $r=0$ to calculate the Pauli potential for the RDA-*m*0 Eq. (71), for the GGA (Ref. 45), and for the PBE2 modified-conjoint GGA functionals. Calculations were performed using our own MAPLE code. For RDA-*m*0, we find

$$v_\theta^{\text{RDA-}m0}(r\to0)=4.5355\times10^5-1.2225\times10^9r+2.1912\times10^{12}r^2+O(r^3), \quad (72)$$

while for the GGA the result is

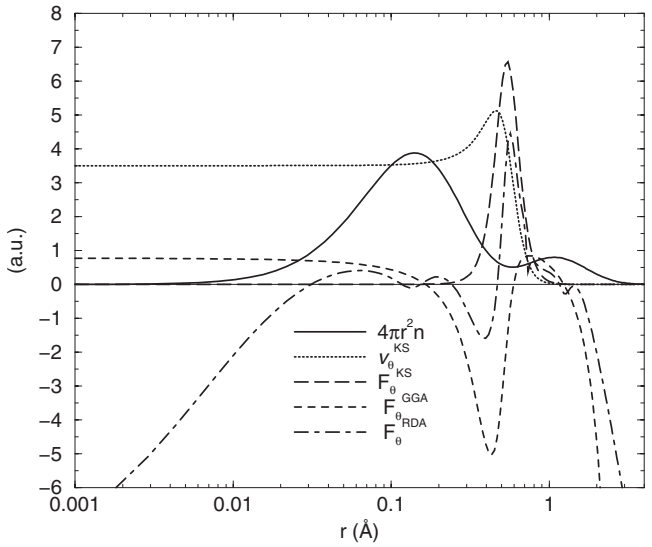

FIG. 9. Numerical KS-LDA density of the Be atom, KS Pauli potential and corresponding enhancement factor, and two approximate enhancement factors.

$$v_\theta^{\mathrm{GGA}}(r\to 0)=\frac{-3.1961}{r}+272.95-1319.1r+3257.5r^2+O(r^3), \tag{73}$$

and for the PBE2 modified-conjoint GGA

$$v_\theta^{\mathrm{PBE2}}(r\to 0)=\frac{0.742}{r}+265.31-1319.6r+3257.1r^2+O(r^3). \tag{74}$$

As expected, the first term in the GGA potential is divergent and negative, while the PBE2 modified-conjoint GGA functional has a divergent but positive first term. The numerical coefficients for the rest of the terms are very close for the GGA and PBE2 modified-conjoint GGA functionals. This closeness is consistent with the analysis in Ref. 30.

Figure 9 shows the KS-LDA Pauli potential for the model Be atom. The value of the potential at the nucleus is approximately 3.5 hartrees. The RDA-*m*0 potential has a finite (and positive) value at nucleus, but it is a strong overestimate, hence, cannot be displayed on the scale of the figure. Further comparison shows that the slope of the RDA-*m*0 Pauli potential at the nucleus has a large negative value, whereas it should be very close to zero (see Fig. 9). To complete the study, three enhancement factors, KS, GGA, and RDA-*m*0, are shown in the same figure. Again, as was seen in Fig. 3 for the SiO molecule, there is an important region where F_θ^{GGA} is negative. The RDA-*m*0 enhancement factor goes negative in a small region near the nucleus and in the tail region. The maximum of the KS enhancement factor near $r\approx 0.75$ Å is reproduced reasonably well by the RDA-*m*0 functional both with respect to position and amplitude.

Though the positivity constraint on F_θ still seems to be highly significant, this numerical study suggests that the failure of the RDA-*m*0 enhancement factor to satisfy that condition everywhere does not necessarily have disastrous consequences on the predicted interatomic forces. Presumably this is because the interatomic forces do not depend explicitly on F_θ, only nuclear position gradients. For the correct prediction of forces the conditions on the corresponding Pauli potential are more important, since it enters explicitly in the equation for forces [see Eq. (5) and discussion in Ref. 7]. (In principle, a functional of the Laplacian of the density might be added to the enhancement factor, whereby the region where the original enhancement factor is negative is removed without altering the predicted interatomic forces.) Supposing that the density and the KS effective potential in Eq. (5) are exact (i.e., taken from the reference KS calculation), error will be introduced solely by the Pauli potential. Since $|\partial n/\partial R_I|$ has large values, the near-nucleus behavior of the Pauli potential is particularly important.

V. DISCUSSION AND CONCLUSIONS

Success for the OF-DFT calculation of quantum forces in molecular dynamics requires a reliable explicit form for T_s. Though previously published GGA-type (conjoint and nearly so) KE functionals yield reasonable KE values, they fail to bind simple molecules even with the correct KS density as input: such functionals produce completely unusable interatomic forces. This poor performance stems from violation of the positivity requirement on the Pauli potential near nuclei. Our first remedy was to constrain conjoint GGA KE functionals to yield positive-definite Pauli potentials. Those functionals generate bound molecules and give semiquantitative interatomic forces. However, they are singular at the nuclear positions, hence, severely overestimate the KS kinetic energy. Examination of the near-nucleus behavior of both original conjoint and modified-conjoint GGA functionals shows that the singularities cannot be eliminated within that simple functional form.

Truncation of the gradient expansion, at higher orders in *s* and *p*, allows us to identify near-nucleus singular behavior and obtain relationships among the coefficients of those truncations that will eliminate such singularities. The resulting reduced density derivatives and related reduced-density-approximation functionals are promising for the simultaneous description of kinetic energies and interatomic forces. A challenge is that there are many possible RDD functionals: so far we do not have a systematic way to select a particular form. Explicit analytic enforcement of the constraints as a means of selection is yet to be done. Also, the RDA-*m*0 form studied here is sufficiently complicated that we do not yet know how to fit it such that all relevant constraints are satisfied.

Two other aspects of the numerical results in Table II relate to exact constraints, hence, deserve brief comment. First, the von Weizsäcker KE is the exact T_s for two-electron singlets. We have not enforced that limit, yet the error from RDA-*m*0 in H_2 is 36 mHartree. Second, violation of *N* representability by an approximate $T_s^{\mathrm{approx}}[n]$ is signaled by $T_s^{\mathrm{approx}}[n]-T_s[n]<0$ for at least one *n*.[62] Five (out of 14) of the RDA-*m*0 entries in Table II have such negative differences. MGGA has none versus all but two being negative for the earlier GGA by Thakkar. However, interpretation of those

computed differences is a bit tricky, in that they do not correspond to the rigorous N-representability-violation test but to $T_s^{\text{approx}}[n]-T_s^{\text{KS,LDA}}[n]$. That is, the reference KS KE is not from the unknown exact density functional but from LDA. With that limitation in mind, the results in Table II are at least suggestive of the notion that the MGGA and RDA-$m0$ functionals are N representable or, in an operational sense, close. It is also important to remember that the narrow goal is a functional that can be parametrized to a small training set which is relevant to the desired materials simulations. This limitation of scope is a practical means for limiting the risks of non-N representability. In addition, we have many RDD forms open for exploration other than RDA-$m0$.

More positively, the RDA-$m0$ functional form shows encouraging signs of transferability outside the range of the training set (recall: only geometries of two molecules and energies of two atoms). A similar fitting procedure was employed in our previous modified-conjoint GGA-type (e.g., PBEν) functionals, which also were constrained to producing a positive-definite Pauli potential (except that the functionals were fitted to energy differences). Despite the small size and limited chemical range of those training sets, the modified-conjoint GGA functionals also exhibit encouraging transferability to periodic solid-state systems containing Si-O bonds, e.g., β-cristobalite or α-quartz; see Ref. 7. Thus, there is basis for the hope that the RDA-type functionals (which differ from the modified-conjoint GGA-type functionals by suppression of nuclear-site singularities in the Pauli potential at the nucleus and by reproducing absolute energies rather than relative energies for deformed geometries of the training set molecules) also will be transferable to extended systems.

We close with a word of caution. Despite this progress, the functional forms examined to this point, e.g., Eq. (71), still may be too simple to provide robust and transferable KE functionals for practical OF-DFT applications. Moreover, the use of RDDs as basic variables in kinetic energy enhancement factors guarantees the finiteness of the corresponding Pauli potential only for those densities which satisfy a generalization of Kato's cusp condition Eq. (59) and does not guarantee the satisfaction of the non-negativity property, Eqs. (16) and (17). The latter constraint must be enforced separately. Nevertheless, the RDA scheme appears quite promising and further development of it is underway.

ACKNOWLEDGMENTS

We acknowledge informative conversations with Paul Ayers, Mel Levy, Eduardo Ludeña, John Perdew, Yan Alexander Wang, and Tomasz Wesolowski. Initial portions of the work by V.V.K., S.B.T., and F.E.H. were supported in part by the U.S. National Science Foundation under Grant No. DMR-0325553. More recent work was supported in part by the U.S. Department of Energy TMS program under Grant No. DE-SC0002139. F.E.H. also acknowledges support from NSF Grant No. PHY-0601758.

APPENDIX A: FUNCTIONAL DERIVATIVES OF F_θ

This appendix provides details relative to derivation of the expressions given in Eqs. (25), (47), and (48). All these formulas follow from an evaluation of an expression of the generic form presented as $v_\theta^{(2i)}(\mathbf{r})$, Eq. (46). That equation is a straightforward expression of the rules for the evaluation of a functional derivative. For clarity in what follows, we restate here the definitions

$$s^2=\frac{\nabla n\cdot\nabla n}{\xi^2 n^{8/3}},\quad p=\frac{\nabla^2 n}{\xi^2 n^{5/3}},\quad t_0([n];\mathbf{r})=c_0 n^{5/3},\quad \text{(A1)}$$

where $\xi^2=4(3\pi^2)^{2/3}$ and $c_0=\frac{3}{10}(3\pi^2)^{2/3}$. We also remind the reader that

$$q=\frac{\nabla n\cdot\nabla\nabla n\cdot\nabla n}{\xi^4 n^{13/3}},\quad q'=\frac{\nabla n\cdot\nabla\nabla^2 n}{\xi^4 n^{10/3}},$$

$$q''=\frac{\nabla^4 n}{\xi^4 n^{7/3}},\quad q'''=\frac{\nabla\nabla n:\nabla\nabla n}{\xi^4 n^{10/3}},\quad \text{(A2)}$$

recall that $A:B\equiv\Sigma_{ij}A_{ij}B_{ji}$. In addition, we introduce the sixth-order reduced density derivatives

$$h=\frac{|\nabla n\cdot\nabla\nabla n|^2}{\xi^6 n^6},\quad h'=\frac{|\nabla\nabla^2 n|^2}{\xi^6 n^4},\quad h''=\frac{(\nabla\nabla^2 n)\cdot(\nabla\nabla n\cdot\nabla n)}{\xi^6 n^5}.\quad \text{(A3)}$$

Finally, we write n instead of the more explicit form $n(\mathbf{r})$, and we note that the derivatives of s^2 and p with respect to n, ∇n, and $\nabla^2 n$ are

$$\frac{\partial(s^2)}{\partial n}=-\frac{8s^2}{3n},\quad \frac{\partial(s^2)}{\partial(\nabla n)}=\frac{2\nabla n}{\xi^2 n^{8/3}},\quad \frac{\partial(s^2)}{\partial(\nabla^2 n)}=0,$$

$$\frac{\partial p}{\partial n}=-\frac{5p}{3n},\quad \frac{\partial p}{\partial(\nabla n)}=0,\quad \frac{\partial p}{\partial(\nabla^2 n)}=\frac{1}{\xi^2 n^{5/3}}.\quad \text{(A4)}$$

Substituting these relations into Eq. (46), and restricting consideration to cases where F_θ depends only on s^2 and p (for which all the terms we need to use are explicitly shown in that equation), we have immediately

$$v_\theta(\mathbf{r})=c_0 n^{2/3}\left[\frac{5}{3}F_\theta-\frac{8}{3}s^2\left(\frac{\partial F_\theta}{\partial(s^2)}\right)-\frac{5}{3}p\left(\frac{\partial F_\theta}{\partial p}\right)\right]$$
$$-\frac{2c_0}{\xi^2}\nabla\cdot\left[\left(\frac{\partial F_\theta}{\partial(s^2)}\right)\frac{\nabla n}{n}\right]+\frac{c_0}{\xi^2}\nabla^2\left(\frac{\partial F_\theta}{\partial p}\right).\quad \text{(A5)}$$

At this point we remark that some terms that would otherwise be expected in Eq. (46) are absent because of the zeros in Eq. (A4).

To proceed further we need to expand the last two terms of Eq. (A5). The first of these terms expands into

$$-2c_0 n^{2/3}\left[\left(\frac{\partial F_\theta}{\partial(s^2)}\right)\left\{\frac{\nabla(n^{-1})\cdot\nabla n+n^{-1}\nabla^2 n}{\xi^2 n^{2/3}}\right\}\right.$$
$$\left.+\left(\frac{\partial^2 F_\theta}{\partial(s^2)^2}\right)\frac{\nabla s^2\cdot\nabla n}{\xi^2 n^{5/3}}+\left(\frac{\partial^2 F_\theta}{\partial p\,\partial(s^2)}\right)\frac{\nabla p\cdot\nabla n}{\xi^2 n^{5/3}}\right].\quad \text{(A6)}$$

Observing now that $\nabla(n^{-1})=-n^{-2}\nabla n$ and that

$$\nabla(s^2) = -\frac{8s^2}{3n}\nabla n + \frac{2\nabla n\cdot\nabla\nabla n}{\xi^2 n^{8/3}},$$

$$\nabla p = \frac{\nabla\nabla^2 n}{\xi^2 n^{5/3}} - \frac{5}{3}\frac{(\nabla^2 n)\nabla n}{\xi^2 n^{8/3}}, \tag{A7}$$

the expression in Eq. (A6) can be brought to the form

$$+2c_0 n^{2/3}\left[(s^2-p)\left(\frac{\partial F_\theta}{\partial(s^2)}\right)+\left(\frac{8}{3}s^4-2q\right)\left(\frac{\partial^2 F_\theta}{\partial(s^2)^2}\right)-\left(q'-\frac{5}{3}s^2 p\right)\left(\frac{\partial^2 F_\theta}{\partial p\,\partial(s^2)}\right)\right]. \tag{A8}$$

Continuing now to the final term of Eq. (A5), we expand the Laplacian obtaining initially

$$\frac{c_0}{\xi^2}\nabla^2\left(\frac{\partial F_\theta}{\partial p}\right) = c_0 n^{2/3}\left[\left(\frac{\partial^2 F_\theta}{\partial(s^2)\,\partial p}\right)\frac{\nabla^2 s^2}{\xi^2 n^{2/3}}+\left(\frac{\partial^2 F_\theta}{\partial p^2}\right)\frac{\nabla^2 p}{\xi^2 n^{2/3}} + \left(\frac{\partial^3 F_\theta}{\partial(s^2)^2\,\partial p}\right)\frac{\nabla s^2\cdot\nabla s^2}{\xi^2 n^{2/3}} + 2\left(\frac{\partial^3 F_\theta}{\partial(s^2)\,\partial p^2}\right)\frac{\nabla s^2\cdot\nabla p}{\xi^2 n^{2/3}}+\left(\frac{\partial^3 F_\theta}{\partial p^3}\right)\frac{\nabla p\cdot\nabla p}{\xi^2 n^{2/3}}\right]. \tag{A9}$$

Using Eq. (A7), we next find

$$\nabla^2 s^2 = -\frac{8}{3}\nabla\cdot\left(\frac{s^2}{n}\nabla n\right)+\frac{2}{\xi^2}\nabla\cdot\left(\frac{\nabla n\cdot\nabla\nabla n}{n^{8/3}}\right) = -\frac{8}{3}\left[-\frac{s^2}{n^2}\nabla n\cdot\nabla n+\frac{\nabla(s^2)\cdot\nabla n}{n}+\frac{s^2}{n}\nabla^2 n\right] + \frac{2}{\xi^2}\left[-\frac{8}{3}\frac{\nabla n\cdot\nabla\nabla n\cdot\nabla n}{n^{11/3}}+\frac{\nabla\nabla n:\nabla\nabla n+\nabla n\cdot\nabla\nabla^2 n}{n^{8/3}}\right],$$

$$\nabla^2 p = \frac{1}{\xi^2}\nabla\cdot\left(\frac{\nabla\nabla^2 n}{n^{5/3}}\right)-\frac{5}{3\xi^2}\nabla\cdot\left(\frac{(\nabla^2 n)\nabla n}{n^{8/3}}\right) = \frac{1}{\xi^2}\left[-\frac{5}{3}\frac{\nabla\nabla^2 n\cdot\nabla n}{n^{8/3}}+\frac{\nabla^4 n}{n^{5/3}}\right] - \frac{5}{3\xi^2}\left[-\frac{8}{3}\frac{(\nabla^2 n)\nabla n\cdot\nabla n}{n^{11/3}}+\frac{(\nabla^2 n)^2}{n^{8/3}}+\frac{\nabla\nabla^2 n\cdot\nabla n}{n^{8/3}}\right],$$

$$\nabla s^2\cdot\nabla s^2 = \frac{64s^4}{9n^2}\nabla n\cdot\nabla n-\frac{32s^2}{3}\frac{\nabla n\cdot\nabla\nabla n\cdot\nabla n}{\xi^2 n^{11/3}}+4\frac{|\nabla n\cdot\nabla\nabla n|^2}{\xi^4 n^{16/3}},$$

$$\nabla s^2\cdot\nabla p = -\frac{8s^2}{3}\frac{\nabla n\cdot\nabla\nabla^2 n}{\xi^2 n^{8/3}}+2\frac{(\nabla\nabla^2 n)\cdot(\nabla n\cdot\nabla\nabla n)}{\xi^4 n^{13/3}}+\frac{40s^2}{9}\frac{(\nabla^2 n)\nabla n\cdot\nabla n}{\xi^2 n^{11/3}}-\frac{10}{3}\frac{(\nabla^2 n)\nabla n\cdot\nabla\nabla n\cdot\nabla n}{\xi^4 n^{16/3}},$$

$$\nabla p\cdot\nabla p = \frac{|\nabla\nabla^2 n|^2}{\xi^4 n^{10/3}}-\frac{10}{3}\frac{(\nabla^2 n)\nabla\nabla^2 n\cdot\nabla n}{\xi^4 n^{13/3}}+\frac{25}{9}\frac{(\nabla^2 n)^2\nabla n\cdot\nabla n}{\xi^4 n^{16/3}}. \tag{A10}$$

Then, combining material from Eqs. (A5) and (A8)–(A10), and introducing the notations in Eqs. (A1)–(A3), we obtain the final result, applicable for any F_θ that depends only on s and p:

$$v_\theta = c_0 n^{2/3}\left[\frac{5}{3}F_\theta-\left(\frac{2}{3}s^2+2p\right)\left(\frac{\partial F_\theta}{\partial(s^2)}\right)-\frac{5}{3}p\left(\frac{\partial F_\theta}{\partial p}\right) + \left(\frac{16}{3}s^4-4q\right)\left(\frac{\partial^2 F_\theta}{\partial(s^2)^2}\right)+\left(\frac{88}{9}s^4+\frac{2}{3}s^2 p-\frac{32}{3}q+2q'''\right)\times\left(\frac{\partial^2 F_\theta}{\partial(s^2)\,\partial p}\right)+\left(\frac{40}{9}s^2 p-\frac{5}{3}p^2-\frac{10}{3}q'+q''\right)\left(\frac{\partial^2 F_\theta}{\partial p^2}\right) + \left(\frac{64}{9}s^6-\frac{32}{3}s^2 q+4h\right)\left(\frac{\partial^3 F_\theta}{\partial(s^2)^2\,\partial p}\right) + \left(\frac{80}{9}s^4 p-\frac{16}{3}s^2 q'-\frac{20}{3}pq+4h''\right)\left(\frac{\partial^3 F_\theta}{\partial(s^2)\,\partial p^2}\right) + \left(\frac{25}{9}s^2 p^2-\frac{10}{3}pq'+h'\right)\left(\frac{\partial^3 F_\theta}{\partial p^3}\right)\right]. \tag{A11}$$

We may now specialize Eq. (A11) to the cases needed in the present work. Taking first F_θ^{GGA}, which has no p dependence, all the terms of Eq. (A11) containing derivatives with respect to p vanish, leaving only the expression previously given as Eq. (25).

Turning next to the specific forms of F_θ discussed in Sec. IV A, we note that $F_\theta^{\mathrm{SGA}}=1+a_2 s^2$ is not only independent of p, but is also linear in s^2, so $\partial F_\theta/\partial(s^2)=a_2$ and $\partial^2 F_\theta/\partial(s^2)^2=0$. This causes v_θ^{SGA} to have the form

$$v_\theta^{\mathrm{SGA}} = c_0 n^{2/3}\left[\frac{5}{3}(1+a_2 s^2)-a_2\left(\frac{2}{3}s^2+2p\right)\right], \tag{A12}$$

which simplifies to the result given in Eq. (47).

Finally, we consider $F_\theta^{(4)}$ as given in Eq. (45). All the third derivatives of F_θ in Eq. (A11) vanish; the first and second derivatives of F_θ have simple forms. We have

$$v_\theta^{(4)} = c_0 n^{2/3}\left[\frac{5}{3}(a_4 s^4+b_2 p^2+c_{21}s^2 p)-\left(\frac{2}{3}s^2+2p\right)(2a_4 s^2+c_{21}p)-\frac{5}{3}p(2b_2 p+c_{21}s^2) + 2a_4\left(\frac{16}{3}s^4-4q\right)+c_{21}\left(\frac{88}{9}s^4+\frac{2}{3}s^2 p-\frac{32}{3}q+2q'''\right) + 2b_2\left(\frac{40}{9}s^2 p-\frac{5}{3}p^2-\frac{10}{3}q'+q''\right)\right]. \tag{A13}$$

Equation (A13) simplifies to the result given as Eq. (48) in the main text.

APPENDIX B: COMPUTATIONAL METHODS

We assess functionals by comparing results from them with those of conventional orbital-dependent Kohn-Sham calculations in the LDA using standard methods described in, for example, Refs. 23 and 63–69. The reference molecular KS calculations were done with a triple-zeta basis with polarization functions.[70–72] All integrals were calculated by a numerical integration scheme that, following Becke,[73] uses weight functions localized near each center to represent the multicenter integrals exactly as a sum of (distorted) atomic integrals. Radial integration of the resulting single-center forms is accomplished by a Gauss-Legendre procedure, while integration over the angular variables is done with high-order quadrature formulas developed by Lebedev and co-workers[74,75] with routines downloaded from Ref. 76. These computations were performed using routines developed by Salvador and Mayer[77] and included in their code FUZZY. The Vosko-Wilk-Nussair LDA (Ref. 68) was used.

Given the KS density, for each OF functional under study we computed the total energy $E^{\text{OF-DFT}}$ from Eq. (3) and the interatomic forces from Eq. (5). The result is a non-self-consistent calculation which tests whether a given OF functional can reproduce $T_s[n_{\text{KS}}]$, or at least $\nabla_{\mathbf{R}} T_s[n_{\text{KS}}]$ if n_{KS} is provided. There is no sense in trying to solve Eq. (4) with an approximate OF functional that cannot pass this test.

*vkarasev@qtp.ufl.edu
†trickey@qtp.ufl.edu

[1] R. Car and M. Parrinello, Phys. Rev. Lett. **55**, 2471 (1985).
[2] D. E. Taylor, V. V. Karasiev, K. Runge, S. B. Trickey, and F. E. Harris, Comput. Mater. Sci. **39**, 705 (2007).
[3] F. H. Streitz and J. W. Mintmire, Phys. Rev. B **50**, 11996 (1994).
[4] M. J. Buehler, A. C. T. van Duin, and W. A. Goddard III, Phys. Rev. Lett. **96**, 095505 (2006).
[5] A. K. Rappe and W. A. Goddard III, J. Phys. Chem. **95**, 3358 (1991).
[6] V. V. Karasiev, S. B. Trickey, and F. E. Harris, Chem. Phys. **330**, 216 (2006).
[7] V. V. Karasiev, S. B. Trickey, and F. E. Harris, J. Comput.-Aided Mater. Des. **13**, 111 (2006).
[8] V. V. Karasiev, R. S. Jones, S. B. Trickey, and F. E. Harris, *New Developments in Quantum Chemistry*, edited by J. L. Paz and A. J. Hernández (Research Signposts, Kerala, 2009), p. 25.
[9] P. Hohenberg and W. Kohn, Phys. Rev. **136**, B864 (1964).
[10] R. G. Parr and W. Yang, *Density Functional Theory of Atoms and Molecules* (Oxford, New York, 1989).
[11] R. M. Dreizler and E. K. U. Gross, *Density Functional Theory* (Springer-Verlag, Berlin, 1990).
[12] L. H. Thomas, Proc. Cambridge Philos. Soc. **23**, 542 (1927).
[13] E. Fermi, Atti Accad. Naz. Lincei, Cl. Sci. Fis., Mat. Nat., Rend. **6**, 602 (1927).
[14] C. F. von Weizsäcker, Z. Phys. **96**, 431 (1935).
[15] E. V. Ludeña and V. V. Karasiev, in *Reviews of Modern Quantum Chemistry: A Celebration of the Contributions of Robert Parr*, edited by K. D. Sen (World Scientific, Singapore, 2002), pp. 612–665.
[16] Y. A. Wang and E. A. Carter, *Theoretical Methods in Condensed Phase Chemistry*, edited by S. D. Schwartz (Kluwer, New York, 2000), Chap. 5, pp. 117–184.
[17] B.-J. Zhou and Y. A. Wang, J. Chem. Phys. **124**, 081107 (2006).
[18] D. García-Aldea and J. E. Alvarellos, Phys. Rev. A **77**, 022502 (2008); J. Chem. Phys. **127**, 144109 (2007) and references in both.
[19] J. P. Perdew and L. A. Constantin, Phys. Rev. B **75**, 155109 (2007).
[20] C. J. Garcia-Cervera, Comm. Comp. Phys. **3**, 968 (2008).
[21] L. M. Ghiringhelli and L. Delle Site, Phys. Rev. B **77**, 073104 (2008).
[22] W. Eek and S. Nordholm, Theor. Chem. Acc. **115**, 266 (2006).
[23] W. Kohn and L. J. Sham, Phys. Rev. **140**, A1133 (1965).
[24] S. B. Trickey, V. V. Karasiev, and R. S. Jones, Int. J. Quantum Chem. **109**, 2943 (2009).
[25] E. Teller, Rev. Mod. Phys. **34**, 627 (1962).
[26] Y. Tal and R. F. W. Bader, Int. J. Quantum Chem. **S12**, 153 (1978).
[27] L. J. Bartolotti and P. K. Acharya, J. Chem. Phys. **77**, 4576 (1982).
[28] J. E. Harriman, in *Density Matrices and Density Functionals*, edited by R. Erdahl and V. H. Smith, Jr. (Reidel, Dordrecht, 1987), pp. 359–373.
[29] M. Levy and Hui Ou-Yang, Phys. Rev. A **38**, 625 (1988).
[30] J. P. Perdew, Phys. Lett. A **165**, 79 (1992).
[31] H. Lee, C. Lee, and R. G. Parr, Phys. Rev. A **44**, 768 (1991).
[32] L. J. Sham, Phys. Rev. A **1**, 969 (1970).
[33] M. Levy, J. P. Perdew, and V. Sahni, Phys. Rev. A **30**, 2745 (1984).
[34] C. Herring, Phys. Rev. A **34**, 2614 (1986).
[35] C. H. Hodges, Can. J. Phys. **51**, 1428 (1973).
[36] I. M. Gelfand and S. V. Fomin, *Calculus of Variations* (Prentice-Hall, Englewood Cliffs, NJ, 1963), p. 42.
[37] G. A. Korn and T. M. Korn, *Mathematical Handbook for Scientists and Engineers* (McGraw-Hill, New York, 1961).
[38] T. Kato, Commun. Pure Appl. Math. **10**, 151 (1957).
[39] W. A. Bingel, Z. Naturforsch. A **18**, 1249 (1963).
[40] R. T. Pack and W. B. Brown, J. Chem. Phys. **45**, 556 (1966).
[41] N. H. March, I. A. Howard, A. Holas, P. Senet, and V. E. Van Doren, Phys. Rev. A **63**, 012520 (2000).
[42] E. S. Kryachko and E. V. Ludeña, *Energy Density Functional Theory of Many-Electron Systems* (Kluwer, Dordrecht, 1990).
[43] The nuclear-electron interaction for the point-nucleus model $v_{\text{ne}}^I(\mathbf{r}) = Z_I/|\mathbf{r}-\mathbf{R}_I|$ is the leading term in v_{KS} Eq. (4) in the limit $\mathbf{r} \to \mathbf{R}_I$. All other terms in v_{KS} are finite at nucleus I and hence are negligible in comparison to v_{ne}^I. Hence, the solution of Eq. (4) in the vicinity of $\mathbf{r}=\mathbf{R}_I$ is a hydrogenlike density. Equation (27) is appropriate also for molecular systems; see Ref. 40.
[44] Zs. Jánosfalvi, K. D. Sen, and Á. Nagy, Phys. Lett. A **344**, 1 (2005).
[45] F. Tran and T. A. Wesolowski, Int. J. Quantum Chem. **89**, 441 (2002).
[46] J. P. Perdew, K. Burke, and M. Ernzerhof, Phys. Rev. Lett. **77**,

3865 (1996).
[47] C. Adamo and V. Barone, J. Chem. Phys. **116**, 5933 (2002).
[48] D. J. Lacks and R. G. Gordon, J. Chem. Phys. **100**, 4446 (1994).
[49] A. E. DePristo and J. D. Kress, Phys. Rev. A **35**, 438 (1987).
[50] A. J. Thakkar, Phys. Rev. A **46**, 6920 (1992).
[51] R. A. King and N. C. Handy, Phys. Chem. Chem. Phys. **2**, 5049 (2000); Mol. Phys. **99**, 1005 (2001).
[52] L. J. Bartolotti (private communication).
[53] D. R. Murphy, Phys. Rev. A **24**, 1682 (1981).
[54] W. Yang, Phys. Rev. A **34**, 4575 (1986).
[55] W. Yang, R. G. Parr, and C. Lee, Phys. Rev. A **34**, 4586 (1986).
[56] P. W. Ayers, R. G. Parr, and A. Nagy, Int. J. Quantum Chem. **90**, 309 (2002).
[57] R. G. Parr and S. K. Ghosh, Proc. Natl. Acad. Sci. U.S.A. **83**, 3577 (1986).
[58] J. E. Harriman, Phys. Rev. A **24**, 680 (1981).
[59] A. Messiah, *Quantum Mechanics* (North-Holland, Amsterdam, 1961), Vol. 1, Appendix B, Sec. 3.
[60] L. A. Constantin and A. Ruzsinszky, Phys. Rev. B **79**, 115117 (2009).
[61] E. Clementi and D. L. Raimondi, J. Chem. Phys. **38**, 2686 (1963).
[62] P. W. Ayers and S. Liu, Phys. Rev. A **75**, 022514 (2007).
[63] J. C. Slater, Phys. Rev. **81**, 385 (1951).
[64] J. C. Slater, Phys. Rev. **82**, 538 (1951).
[65] J. C. Slater, J. Chem. Phys. **43**, S228 (1965).
[66] R. Gáspár, Acta Physiol. Hung. **3**, 263 (1954).
[67] B. Y. Tong and L. J. Sham, Phys. Rev. **144**, 1 (1966).
[68] S. H. Vosko, L. Wilk, and M. Nusair, Can. J. Phys. **58**, 1200 (1980).
[69] D. M. Ceperley and B. J. Alder, Phys. Rev. Lett. **45**, 566 (1980).
[70] A. Schäfer, H. Horn, and R. Ahlrichs, J. Chem. Phys. **97**, 2571 (1992).
[71] A. Schäfer, C. Huber, and R. Ahlrichs, J. Chem. Phys. **100**, 5829 (1994).
[72] From the Extensible Computational Chemistry Environment Basis Set Database, Version 02/25/04, Molecular Science Computing Facility, Environmental and Molecular Sciences Laboratory, Pacific Northwest Laboratory, P.O. Box 999, Richland, Washington 99352, USA, funded by the U.S. Department of Energy (contract DE-AC06-76RLO). See http://www.emsl.pnl.gov/forms/basisform.html
[73] A. D. Becke, J. Chem. Phys. **88**, 2547 (1988).
[74] V. I. Lebedev and D. N. Laikov, Dokl. Akad. Nauk **366**, 741 (1999).
[75] V. I. Lebedev and D. N. Laikov, Dokl. Math. **59**, 477 (1999).
[76] Computational Chemistry List (CCL) Archives (http://www.ccl.net/).
[77] P. Salvador and I. Mayer, J. Chem. Phys. **120**, 5046 (2004).